



Grant agreement No. 640979

ShaleXenvironment

Maximizing the EU shale gas potential by minimizing its environmental footprint

H2020-LCE-2014-1

Competitive low-carbon energy

D12.10

Material for Academic Course

WP 12 – Dissemination

| | |
|--------------------------------|---|
| Due date of deliverable | 31/08/2018 (Month 36) |
| Actual submission date | 03/09/2018 (Month 37) |
| Start date of project | 1 st September 2015 |
| Duration | 36 months |
| Lead beneficiary | Geomecon |
| Last editor | Alberto Striolo |
| Contributors | UCL, CSGI, ARMINES, UoM, NCSR'D, UA, HIPC, ICPF, Geomecon |
| Dissemination level | Public (PU) |



This Project has received funding from the European Union's Horizon 2020 research and innovation programme under grant agreement no. 640979.

Disclaimer

The content of this deliverable does not reflect the official opinion of the European Union. Responsibility for the information and views expressed herein lies entirely with the author(s).

History of the changes

| Version | Date | Released by | Comments |
|----------------|-------------|-----------------------|--|
| 1.0 | 30-07-2018 | Alberto Striolo (UCL) | Collected contributions from partners and made editorial changes |
| 1.1 | 20-08-2018 | Alberto Striolo (UCL) | Collected revised contributions from partners when needed |
| 1.2 | 31-08-2018 | Alberto Striolo (UCL) | Finalized document, edited and combined all contributions |

Table of contents

| | | |
|----|--|-----------|
| 1. | Introduction..... | 7 |
| | 1.1 General context | 7 |
| | Why is the debate so fierce? | 7 |
| | Do we need shale gas in the fist place?..... | 7 |
| | How is shale gas produced? | 8 |
| | Has there been a technology breakthrough recently?..... | 9 |
| | What can modern practitioners do? | 10 |
| | So, is Shale Gas a Friend, or a Foe? | 10 |
| | 1.2 Deliverable objectives | 10 |
| 2. | Methodological approach | 11 |
| 3. | Summary of activities and research findings..... | 12 |
| | 3.1 Advanced Imaging and Geomechanical Characterisation..... | 12 |
| | 3.1.1 Scientific questions and environmental impacts addressed | 12 |
| | 3.1.2 Main results achieved during the project..... | 12 |
| | 3.1.2.1 Shale microstructure governs mechanical properties..... | 12 |
| | 3.1.2.2 Multi-scale nature of pore size, structure, networks and potential flow paths..... | 13 |
| | 3.1.2.3 Relations between tomographic and geomechanical observations | 14 |
| | 3.1.3 Next steps and social impacts..... | 16 |
| | 3.1.4 Selected publications resulting from this work | 16 |
| | 3.1.5 References | 17 |
| | 3.2 Modelling of Confined Fluids | 18 |
| | 3.2.1 Scientific questions addressed and environmental impacts addressed | 18 |
| | 3.2.2 Main results achieved during the project..... | 18 |
| | 3.2.2.1 Water based fracturing fluids in clay mesopores | 18 |
| | 3.2.2.2 Shale gas in type II kerogen | 21 |
| | 3.2.3 Next steps and social impacts..... | 22 |
| | 3.2.4 Selected publications resulting from this work | 23 |
| | 3.3 New Formulations to Reduce the Environmental Footprint | 26 |
| | 3.3.1 Scientific questions and environmental impacts addressed | 26 |
| | 3.3.1.1 Where we started from: the existing formulations..... | 26 |
| | 3.3.2 Main results achieved during the project..... | 27 |
| | 3.3.2.1 Polysaccharide-based Formulations..... | 27 |
| | 3.3.2.2 ViscoElastic Surfactant (VES) – based formulations | 29 |
| | 3.3.2.3 “Smart” Responsive Formulations | 30 |
| | 3.3.2.4 NORM reduction strategies..... | 32 |
| | 3.3.3 Next steps and social impacts..... | 32 |
| | 3.3.4 Selected publications resulting from this work | 33 |
| | 3.3.5 References | 33 |
| | 3.4 Analytical Models and Software | 35 |
| | 3.4.1 Scientific questions and environmental impacts addressed | 35 |
| | 3.4.2 Main results achieved during the project..... | 36 |
| | 3.4.2.1 Microscopic transport modelling | 36 |
| | 3.4.2.2 Geomechanical modelling and permeability simulation..... | 37 |
| | 3.4.2.3 Simulation of fracture network evolution by hydraulic stimulation | 38 |

| | | |
|-------------|---|-----------|
| 3.4.2.4 | Reservoir scale analysis | 39 |
| 3.4.3 | Next steps and social impacts..... | 40 |
| 3.4.4 | Selected publications resulting from this work | 41 |
| 3.4.5 | References | 41 |
| 3.5 | Synthesis and Characterisation of Engineered Materials | 43 |
| 3.5.1 | Scientific questions and environmental impacts addressed | 43 |
| 3.5.2 | Main results achieved during the project..... | 43 |
| 3.5.3 | Next steps and social impacts..... | 45 |
| 3.5.4 | Selected publications resulting from this work | 46 |
| 3.6 | Optimisation of Shale Gas Water Treatment | 47 |
| 3.6.1 | Introduction and Objectives | 47 |
| 3.6.2 | Optimal Shale Water Pre-Treatment..... | 48 |
| 3.6.3 | Shale Water Desalination | 49 |
| 3.6.4 | Shale Water Management..... | 50 |
| 3.6.5 | Life Cycle Assessment | 51 |
| 3.6.6 | Next Steps and social impacts | 52 |
| 3.6.7 | Selected publications resulting from this work | 52 |
| 3.7 | Development of a reliable wellhead blowout model and its applicability to a case study..... | 54 |
| 3.7.1 | Scientific questions and environmental impacts addressed | 54 |
| 3.7.2 | Main results achieved during the project..... | 54 |
| 3.7.3 | Next steps and social impacts..... | 55 |
| 3.7.4 | Selected publications resulting from this work | 55 |
| 3.8 | Development of a Methodology for quantifying the likelihood of natural and induced seismic activity due to hydraulic fracturing and its application to case studies..... | 57 |
| 3.8.1 | Scientific questions and environmental impacts addressed | 57 |
| 3.8.2 | Main results achieved during the project..... | 58 |
| 3.8.3 | Next steps and social impacts..... | 58 |
| 3.8.4 | Selected publications resulting from this work | 59 |
| 3.8.5 | References | 59 |
| 3.9 | Life Cycle Assessment and Shale Gas | 60 |
| 3.9.1 | What is Life Cycle Assessment?..... | 60 |
| 3.9.2 | Why Life Cycle Assessment?..... | 60 |
| 3.9.3 | Life Cycle Assessment and shale gas | 61 |
| 3.9.4 | The LCA standard framework | 61 |
| 3.9.4.1 | Goal and Scope definition | 62 |
| 3.9.4.2 | Life Cycle Inventory | 64 |
| 3.9.4.3 | Life Cycle Impact Assessment..... | 65 |
| 3.9.4.4 | Life Cycle Interpretation..... | 67 |
| 3.9.5 | Reading material..... | 68 |
| 3.9.6 | References | 69 |
| 3.10 | Worthiness and Social License to Operate (SL2O) | 70 |
| 4. | Conclusions and future steps | 72 |
| 5. | Publications resulting from the work described..... | 72 |

List of figures

| | |
|--|----|
| Figure 1: Composition and triaxial compressive strength (a) and static Young's modulus (b) of various shale samples..... | 13 |
| Figure 2: 3D microstructure of a Lower Bowland Shale sample B6. | 14 |
| Figure 3: Pore size distribution in Bowland B6 sample, quantified from FIB images. | 14 |
| Figure 4: Tomograph cross-sections of a Haynesville shale sample cored parallel to bedding. | 16 |
| Figure 5: Atomic density profiles along the axis normal to the kaolinite (001) surfaces for the systems with and without the protonated citric acid (H ₃ A). a) NaCl, b) CsCl, c) SrCl ₂ and d) BaCl ₂ . The RI and RIII regions of each diagram correspond to the gibbsite and siloxane surfaces, respectively..... | 19 |
| Figure 6: Atomic density profiles along the axis normal to the (010) montmorillonite surfaces for the systems containing 1480 H ₂ O molecules, 6 NaCl (0.1M), and 4 BaCl ₂ /SrCl ₂ (0.07M). | 20 |
| Figure 7: Ratios between confined and bulk concentration of Na ⁺ and Cl ⁻ electrolytes as a function of pore width..... | 21 |
| Figure 8: Maximum component of the diffusion coefficient of pure methane in a variety of type II kerogen models as function of the limiting (primary horizontal axis) and maximum (secondary horizontal axis) pore diameters of the structure at 298.15 K and 250 atm. A linear trend line is fitted to the D vs LPD points. | 22 |
| Figure 9: Influence of some specific salts on Sodium Hyaluronate viscosity. | 27 |
| Figure 10: Rheological behaviours of Guar Gum, Sodium Hyaluronate and HydroxypPropyl Cellulose both in water and in high salinity conditions (Shale Water). | 28 |
| Figure 11: on the left, flow curves of GG, HPC and SH in water and in the simultaneous presence of SW and saponin; on the right, flow curves of GG, HPC and SH in water and in the simultaneous presence of SW and sodium citrate..... | 28 |
| Figure 12: Precipitation of CaSO ₄ in SH formulation. The numbers from 0 to 6 indicate the different anti-scale agent added: 0-no anti-scale agent, 1-polyaspartate, 2-low molecular weight polyglutamate, 3-high molecular weight polyglutamate, 4-low molecular weight polyacrylate, 5-intermediate molecular weight polyacrylate, and 6-high molecular weight polyacrylate. All the scale bars are 100 μm. | 29 |
| Figure 13: on the left, flow curves of VES formulations at different sodium oleate (NaOL) concentration and fixed KCl content; on the right, zero-shear viscosities of 13% w. NaOL at various KCl concentrations; bottom, flow curves acquired on NaOL 13% w. + KCl 4% w. at different applied pressures. | 30 |
| Figure 14: on the top left, flow curves of GG formulation, both with and without the addition of CB, acquired at different temperatures ranging from 25 °C to 60 °C; on the top right, flow curves of NaOL + CB formulation acquired at different temperatures ranging from 25 °C to 60 °C; on the bottom left, flow curves of SH + CB and HPC + CB formulations acquired both previous and after the electrical treatment; on the bottom right, flow curves of NaOL + CB formulation acquired both previous and after the electrical treatment. | 31 |
| Figure 15: flow curves acquired on NaOL/KCl formulations, both with and without the addition of azorubine. Continuous and dotted lines represent non-irradiated and irradiated samples, respectively..... | 31 |
| Figure 16: Optical microscopy images about the precipitation of CaCO ₃ , SrCO ₃ and BaCO ₃ when a magnetic field of ≈0.4 T is applied at 25 °C (top) and at 60 °C (bottom). All the scale bars are 100 μm. | 32 |
| Figure 17: Increasing number of fractures and fracture density with increasing area (left) and increasing bulk permeability with increasing investigated scale following a logarithmic law for vertical and horizontal flow (right). | 37 |
| Figure 18: Fracture network extension examples. The fracture domains are 5x5, 10x10 and 15x15m and depicted in relative scale. The colour code indicates fluid overpressure in fractures, blue: 0 MPa and red: 11 MPa..... | 38 |
| Figure 19: [top left] Model for the numerical simulations. The model consists of a cap- (light grey on faults) and a reservoir rock mass (dark grey) that are cut by permeable faults. Injection of cold water is applied through an open hole section in the southern compartment (blue line) while production is conducted in the northern compartment (red line). [top right] Results of the simulation with poroelastic rock mass. Large areas of the southern fault become destabilised during injection (red), while the northern fault is stabilised by production (green). Stability on the faults is not aligned with pore pressure (isolines). The rock mass shows some increase in differential stresses at the injection well and close to the faults (red isobar). In the production compartment | |

large volumes get depressurised as indicated by the blue isobar. [bottom left] Results from simulation with a non-homogeneous fracture containing rock mass highlight reduced areas of stability change on faults. [bottom right] The results of simulation of the influence of a hydraulic fracture treatment show comparable fault stability pattern compared to the homogeneous solution (top right) but with altered influence on rock mass. 40

Figure 20: Schematic representation of ADOR process. ‘A’ stands for assembly of the parent UTL structure, ‘D’ – disassembly to IPC-1P zeolite precursor, ‘O’ – organizing by intercalation of organics, and ‘R’ – reassembly by calcination (in this example to IPC-4 (PCR))..... 43

Figure 21: Isothermic heats of adsorption of carbon dioxide on UTL and IPC-n zeolites. 45

Figure 22: Typical profile of water flow and TDS vs time. Based on data from Marcellus Shale (USA) 48

Figure 23: a) Environmental impacts by section for the extraction of shale gas. b) Comparison of the environmental impacts of the studied desalination technologies by damage subcategory. 51

Figure 24: Incident heat flux contours at the ground level around vertical flame formed from the wellhead, predicted at 0.5, 2, 10 and 50 seconds following blowout under no wind conditions..... 55

Figure 25: Physical mechanisms that could induce seismicity in hydraulic fracturing, (left): 1) Injection well drilled directly into fault, 2) hydraulic fracture directly intersects fault, 3) fluid flow through existing fractures, 4) through more permeable rock strata above or below shale formations, or through bedding planes that interface the rock strata; (right) changes in the stress field brought about by changes in volume or mass loading transmitted to the fault poroelastically (After Davies et al., 2013 and Schultz et al., 2017). 58

Figure 26: Phases of Life cycle Assessment, adapted from ISO 14040 (ISO, 2006a). 62

Figure 27: System boundary for shale gas within the SXT project. Yellow boxes represent the hydraulic fracturing process, grey boxes identify the conventional processes and the blue boxes refer to the activities of the background system. 64

Figure 28: Hot-spot analysis for the global warming category relative to the production of 1 MJ of shale gas. . 68

Figure 29: Sensitivity analysis for the global warming category relative to the production of 1 MJ of shale gas. 68

List of tables

Table 1: Examples of LCIA terms (adapted from ISO, 2006a)) 66

1. Introduction

1.1 General context

Shale gas attracts large attention and creates strong divisions. In North America it triggered an economical renaissance. In countries such as China and Argentina, where enormous shale gas potentials could help achieve energy independence, the industry is pouring large investments. In Europe, the debate quickly escalates and the landscape is fragmented. France, *e.g.*, banned shale gas, Poland would like to produce it but technical problems are in the way, the UK is experimenting with it and the public is divided. When the ShaleXenvironment project was announced, one UCL colleague found molasses on his office door, and we were unceremoniously invited to '*stop doing public relations for big oil*'.

Why is the debate so fierce?

Although modern society seeks alternatives to oil and gas, the path is not clear. The February issue of *The Chemical Engineer* reported that '*France's parliament has passed a law banning the production of oil and gas in the country's territories from 2040*'; that '*Trump proposes opening most US waters to drilling*'; and that '*Shell will redevelop the Penguins oil and gas field*', in the North Sea. Shale gas could provide energy for the years to come, but it is a fossil fuel and as such it is not renewable.

Producing shale gas has inherent risks, which include, but are not limited to induced seismicity, increased heavy-duty surface traffic, chemicals and hydrocarbons spills, use of large amounts of fresh water, methane migration in the sub-surface and groundwater water contamination. Drilling the wells is complex; hydrocarbons are flammable and explosive. Most oil and gas operations face similar risks, and in some tragic circumstances fatalities have occurred in the sector. Engineers should continue to design preventive, mitigating and remediation procedures to contain such risks. The highest standards of safety must be implemented in any industrial operation, including the production of shale gas. Yet, the risks exist.

But let us step back, and consider whether shale gas could be an opportunity for a technological renaissance. Below, some possible future developments in fundamental and applied research and in education are briefly proposed.

Do we need shale gas in the first place?

The International Energy Agency (IEA) estimates that oil and gas demand, worldwide, will continue to rise at least for 20 more years. While the society pursues the development of renewable energy sources, one notices that shale formations are ubiquitous. The IEA estimated that shale formations are present in 42 countries. The estimated recoverable reserves in China alone [1,115 trillion cubic feet, tcf] could supply the UK for over 350 years at current demand. The Department for Business, Energy & Industrial Strategy reported that the UK consumed ~ 3 tcf of natural gas in 2016: ~ 33% of it produced electricity, 35% was

used domestically and ~17% industrially. More than half of the natural gas consumed in the UK is imported.

How is shale gas produced?

Two major innovations enabled the shale gas revolution. One involves 'directional drilling': the wells extend horizontally from the well pad. The other is hydraulic fracturing, which attracts public's ire. Stanolind Oil and Gas Operation pioneered hydraulic fracturing in the 1940's in Kansas, USA. Millions of 'frac jobs' have now been performed on oil and gas wells. By pumping water, or other fluids, hydraulic fracturing creates a fractures network within an otherwise impermeable formation. Sand and other 'proppants' maintain the fractures open to facilitate gas production.

Many fundamental challenges still exist. It is estimated that only 15-20% of the gas in place is produced. The rest remains within the shale formation. How could this latter gas be produced? Could, *e.g.*, CO₂ enhance production, yielding the added benefit of permanent carbon sequestration?

It is difficult to precisely quantify the amount of hydrocarbons present within a formation. New tools are needed to measure gas adsorption at pressure and temperature conditions typical of the geological formation, to visualize the existing pore network within a shale rock, to test the mechanical properties of the rocks, and the cracks propagation when the rock is fractured.

Advanced instruments such as synchrotrons or X-ray computer tomographs are required to visualize the 3D pore network in shale rock samples. While all shale rocks are different, their pore networks are not isotropic and lack connectivity.

Analysis of such data reveals an important feature: many of the pores have dimensions comparable to that of fluid molecules. When water, methane, CO₂, etc., are confined in such narrow pores, it is no longer possible to apply our thermodynamic understanding of bulk fluids for predicting fluid phase behaviour, mutual solubility, or transport. This opens up a whole new field of fundamental investigations, which require experimental, theoretical and computational approaches for better quantifying the properties of confined fluids.

It is essential to predict the transport of fluids through sub-surface formations. Given the heterogeneity of shale rocks, the narrow pores typically present, and the lack of extensive connectivity within the pore network, existing analytical and computational approaches tend to fail, for different reasons. Recently, stochastic approaches have been attempted, yielding promising results.

Any progress in the fundamental research topics just summarized will bear fruit for cutting-edge applications familiar to chemical engineers: carbon storage, geothermal energy

production, prevention of environmental contamination, catalysis, liquid and gas separations, energy storage, etc.

Fresh water was used in the first hydraulic fracturing operations, mixed with chemicals such as viscosity modifiers. Fresh water is precious and its usage should always be limited, especially in areas affected by water scarcity. While some progress has been made, the community could thrive through innovating fracturing fluids. If the new fluids tolerated salt, not only less fresh water would be needed, but also water produced from the fractured wells could be re-used. Innovative fluids could contain only bio-degradable chemicals, *e.g.*, sugars, could precipitate undesired compounds in the sub-surface, which would reduce environmental impact, and could contain 'smart' particles to extract higher molecular weight hydrocarbons. These research ideas are at the boundary between Chemical Engineering, Chemistry, Environmental Sciences, Materials Science and Nanotechnology. We should however not forget Economics and Risk Prevention and Mitigation: innovation needs to be environmentally safe and cost-effective.

In most oil and gas operations, large amounts of water are produced, which need to be treated. Depending on the shale formation, produced water can contain large amounts of salt, naturally occurring radioactive materials (NORM), organics and solid particles. Depending on the amount of water produced, on its composition, on the final use, and on the well location, different technologies will be optimal. When the operations are remote, solar power might operate water purification processes, as well as the wells themselves. When appropriate, mobile water treatment plants could be adopted. When several wells are nearby, automated processes that collect water, treat it, and redistribute it via pipelines could reduce water and energy consumption, as well as truck traffic at the surface.

Has there been a technology breakthrough recently?

The technology continues to evolve. For example, one horizontal well, drilled in 2011 and fractured 15 times, produced in 1 year as much gas as a typical vertical well, drilled in 1996 and fractured once, produced in 15 years.

The plunging oil price of 2014-2015 caused a massive shock. The break-even point for producing North American unconventional oil was ~ \$60 per barrel in 2014: highly profitable operations became economically unsustainable when the oil price dropped to \$50 or below. 163,000 jobs were lost in the sector, approximately 30% of the work force during peak production. This shock forced the industry to innovate, and the break-even point became ~\$35 a barrel for unconventional operations in Texas in 2017. Shale gas operations are again profitable in the USA, but they have changed. A modern control room located in an urban environment now operates, remotely, oil and gas wells located miles away. Multi-disciplinary teams comprised of engineers, geoscientists, and computer scientists lead the operations. Remotely controlled and automated machineries perform most of the needed tasks: drilling rigs move autonomously, drones monitor the operations and sample air

composition, automated instruments detect and localize eventual gas leaks. Multiple wells are drilled parallel to each other, many fracturing jobs are conducted on the same well, big data and Artificial Intelligence are used to replicate the procedures from the best-performing wells on new operations, interpreting and sometimes predicting rock properties. For similar innovations to continue revolutionise the sector while ensuring that the processes are environmentally safe, future Chemical Engineers will have to interact with Electronic Engineers, Geologists, Computer Scientists, Safety Engineers, and other professional figures.

What can modern practitioners do?

Answering the fundamental questions listed above can contribute to reduce the environmental impacts of shale gas production. Although much can be done building on our traditional background, the recent past shows that truly transformative innovations are achieved at the boundaries between multiple diverse disciplines. Are we training engineers for this challenge and opportunity? As a first step to a multi-disciplinary education in the energy and resources sector, UCL introduced the MSc in Global Management of Natural Resources. The students master material from Geology, Engineering, Management and Social Sciences. The latter is required to acquire the social license to operate, for a complex industrial activity such as shale gas production to take place.

So, is Shale Gas a Friend, or a Foe?

This overview is mostly focused on the scientific and technological challenges that have surfaced because, in part, to shale gas. However, deciding whether to embark on a practical operation is complicated. Many are the stakeholders, who should all be part of decision-making: those living near a potential site, government, companies and operators, possibly others, who exercise competing demands for limited resources such as water or roads.

Although as scientists we advocate that decisions should be supported by hard evidence, the recent political climate suggests some distrust with regards to science and technology. Collectively, we should demonstrate that evidence-based discourses can lead to progressive policies and regulations that improve the standard of living of all while safeguarding the environment, support economic development and create jobs while not exposing communities to un-necessary risks. Life Cycle Assessment, LCA, promises to be a useful tool for informing policy makers building on scientific evidence. LCA could quantify environmental, financial and societal impacts of a given technology. One could apply LCA to any technology that could provide the 3 tcf of natural gas required by the UK, and identify the one that minimises the overall environmental and societal impacts. In the event that such technology is not the most economical, will the society accept to bear the costs?

1.2 Deliverable objectives

Work Package 12 is charged with disseminating widely the results from the H2020 consortium ShaleXenvironment. One of the goals of our dissemination plan is to leave a

long-lasting legacy. Deliverable 12.10 has the objective of providing materials that could be used in introductory academic modules focused on the various aspects of shale gas exploration and production that were explored by the ShaleXenvironmentT consortium.

2. Methodological approach

Each of the technical Work Packages provided short summaries of the activities conducted. The details of the activities are discussed at length within the technical Deliverables, to which the interested Reader is referred to for further technical details. We provide below a sequential summary, which addresses: (1) state of the art; (2) a selection of major results accomplished during the ShaleXenvironmentT project; (3) identification of possible future directions; (4) a few suggested articles for further reading. This material could be developed, in the future, as a book.

3. Summary of activities and research findings

3.1 Advanced Imaging and Geomechanical Characterisation

3.1.1 *Scientific questions and environmental impacts addressed*

This Work Package aims to provide careful experimental characterisation of the shale rock samples extracted from formations throughout Europe, studying experimental fracture formation and propagation, as well as fluid behaviour in core samples. The team members have developed new technologies to push the existing limits.

The improved understanding of microstructure, pore network and mechanical properties in shales from this project will allow assessment of more efficient gas extraction processes. The imaging and quantification of fracture initiation and propagation will enhance the gas shale recovery and also improve the prediction of the environmental impact on earthquakes and leakage in ground water.

3.1.2 *Main results achieved during the project*

3.1.2.1 *Shale microstructure governs mechanical properties*

The long-time productivity of a well in unconventional hydrocarbon formations such as shale gas plays is strongly influenced by the relationships between the shale microstructure and the stress induced by hydraulic stimulation, which govern for example the stress-induced fracture-healing rate of artificially generated cracks (Rutter and Mecklenburgh, 2017). The fracture-healing rate of those rocks depends on different factors like microstructure, porosity and mineralogy, differential stress, pressure and temperature.

Measured stress-strain curves of tested samples are shown in **Figure 1**, revealing that Posidonia and Alum shales, as well as one porous and TOC-rich Upper Bowland shale, are relatively weak with low Triaxial Compressive Strength (TCS) and pronounced inelastic deformation. In comparison, the Bowland shale is much stronger and more brittle, almost independently of the relative carbonate and quartz/feldspar/pyrite (QFP) content. In general, shales with a low fraction of 'weak' phases reveal high TCS (**Figure 1a**), in particular if the carbonate content (and not the QFP fraction) is also high. The static Young's moduli increase with increasing strength as observed in other shales (Rybacki et al., 2015). Similar to TCS, high E-values were obtained for samples with low fraction of weak phases and particularly with high carbonate content (**Figure 1b**). Our results suggest that the triaxial compressive strength and static Young's modulus of shales depend on whole rock composition, where dense rocks with a low amount of TOC and phyllosilicates, but relatively high carbonate fraction, display the highest values and preferentially brittle deformation behaviour. Compared to other European shales, the Bowland shale formation represents a strong and brittle shale type that may show a good 'frackability' and low fracture-healing rate, but contains also a low TOC content.

In summary, using traditional characterisation techniques, the relative values of total organic content (TOC), porosity, petrophysical and phase fraction quantities, mechanical properties, and permeability were measured for selected shale samples. The obtained experimental values, and the correlations between them both increase our understanding of the fundamental mechanisms responsible of fracture formation and propagation in shale rocks by hydraulic stimulation, and they also provide the critical inputs for models of this behaviour. Via improved understanding and modelling, the community will be able to better account for the environmental footprint of these processes.

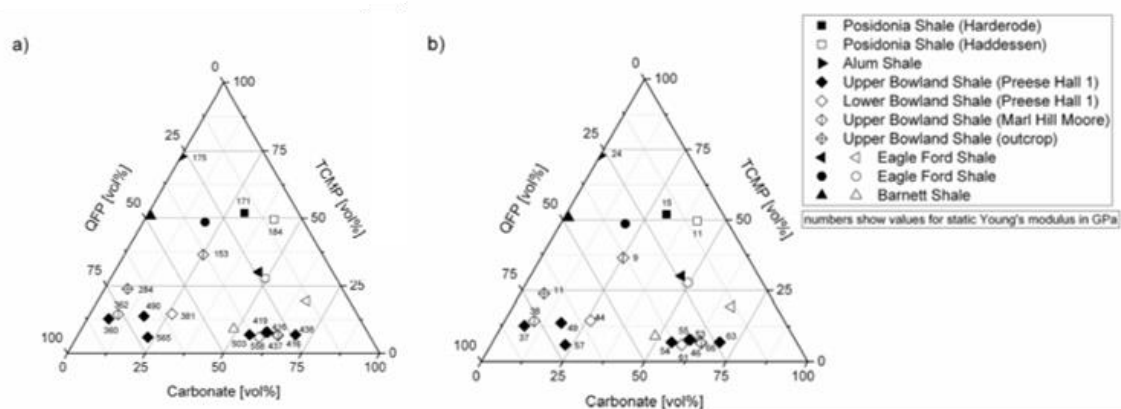


Figure 1: Composition and triaxial compressive strength (a) and static Young's modulus (b) of various shale samples.

3.1.2.2 Multi-scale nature of pore size, structure, networks and potential flow paths

A range of imaging techniques have been used to cover multiple scales from mm to nm (SEM, XCT and FIB) in our attempts to quantify pore size, structure, networks and potential flow paths in selected samples. The microstructure and the porous network of the Bowland shale samples are highly heterogeneous. Based on the large volume of data, the heterogeneity of all porous phases has been quantified (**Figure 2**). Some specific organic matter particles are selected for higher-resolution quantification, and the distribution and connectivity of two common organic matter, small irregular particles and large piece of organic matter, are analysed. Pores are quantified based on their relationship to the porous phase. Pores in the selected samples range 20 nm – 1 μ m in size, which was quantified in 3D FIB images at nano-scale. No continuously interconnected network is detected at this image resolution, but potential flow paths may exist within porous phases below the experimental resolution. Pores are observed to be associated with two porous phases, organic matter and minerals (clays and carbonates). Pores in organic matter have larger sizes, more number and higher connectivity locally in organic rich areas, while mineral pores have wider distribution in the whole sample. The spatial distributions of these porous phases were quantified in synchrotron tomography images at micro-scale. Organic matter shows more elongated particles shapes, but lower content and lower connectivity than minerals. Hydraulic

fracturing can produce cracks inside samples to provide more efficient pathways for the oil/gas in shales. Large hydraulic fractures are perpendicular to bedding and thin fractures follow the bedding showing a multi-scale and complex fracture network.

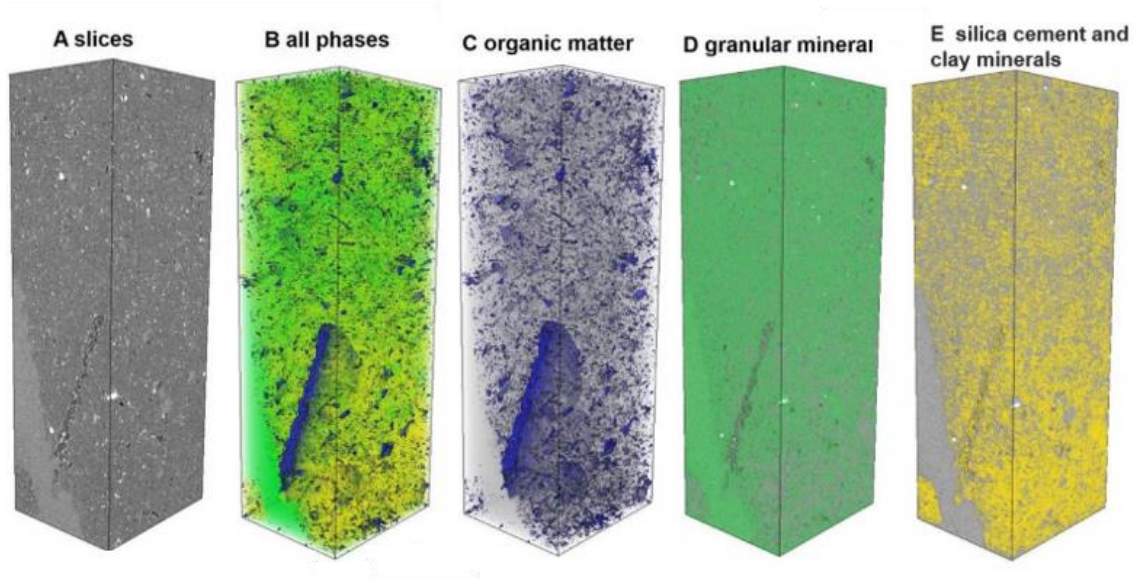


Figure 2: 3D microstructure of a Lower Bowland Shale sample B6.

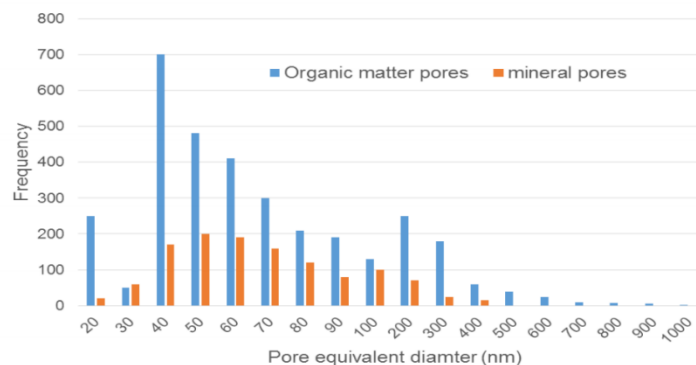


Figure 3: Pore size distribution in Bowland B6 sample, quantified from FIB images.

3.1.2.3 Relations between tomographic and geomechanical observations

Fracture growth and sealing in the subsurface are often complex, yielding tortuous pathways showing significant horizontal and vertical extent (Fisher and Warpinski, 2012; Thiercelin et al., 1987). Hydraulic fracturing experiments, at either constant strain rate or constant stress condition, were performed to understand the geomechanical properties of shales. Synchrotron-based time-resolved X-ray tomography (4D XCT) allows for the understanding of the local conditions around a fracture as it develops and seals (Figuroa Pilz et al., 2017). The relations between tomographic and geomechanical observations therefore improves the understanding of shale mechanical properties significantly and have strong implications for reservoir conditions and sweet spot identification.

The in-situ imaging experiments were conducted on samples manufactured in two orientations with respect to the bedding planes. The confining pressure was applied gradually, with regular pauses to record tomographs of the sample material under increasing confinement. Once the desired confining pressure was reached, the pressurisation system was reconnected and used to increase the borehole pressure, simulating a rise in fluid injection pressure. Injection pressure was raised gradually, with pauses for tomographic imaging. Once the breakdown pressure was reached, the fracture growth (and resultant pressure drop) was found to be rapid and uncontrolled. The injection pressure was a function of the volume of fluid injected. After failure, the injection pressure was lowered to zero, and the confining pressure was raised, in order to image the pressure-driven closure of fractures (**Figure 4**). Fractures occur in the borehole-parallel orientation in bedding-parallel samples of all materials. In bedding-perpendicular samples, fractures only develop in the borehole-parallel orientation in the unlaminated materials. In materials where layering is present, the fractures were commonly seen to grow in a borehole-perpendicular orientation, so as to follow the layering in the material. Breakdown pressure during these experiments was found to increase with confining pressure, but was seen to be isotropic between the two sample orientations, and not strongly sensitive to the different material. At ambient conditions these microcracks have a strong effect on the propagation of fractures, but this is suppressed by the microfracture closure at elevated. Existing fractures were observed in some of the initial sample materials. Pre-existing fractures were generally more numerous in the more laminated materials. There are small connecting cracks (either pre-existing or generated during breakdown) that are below the resolution of our images.

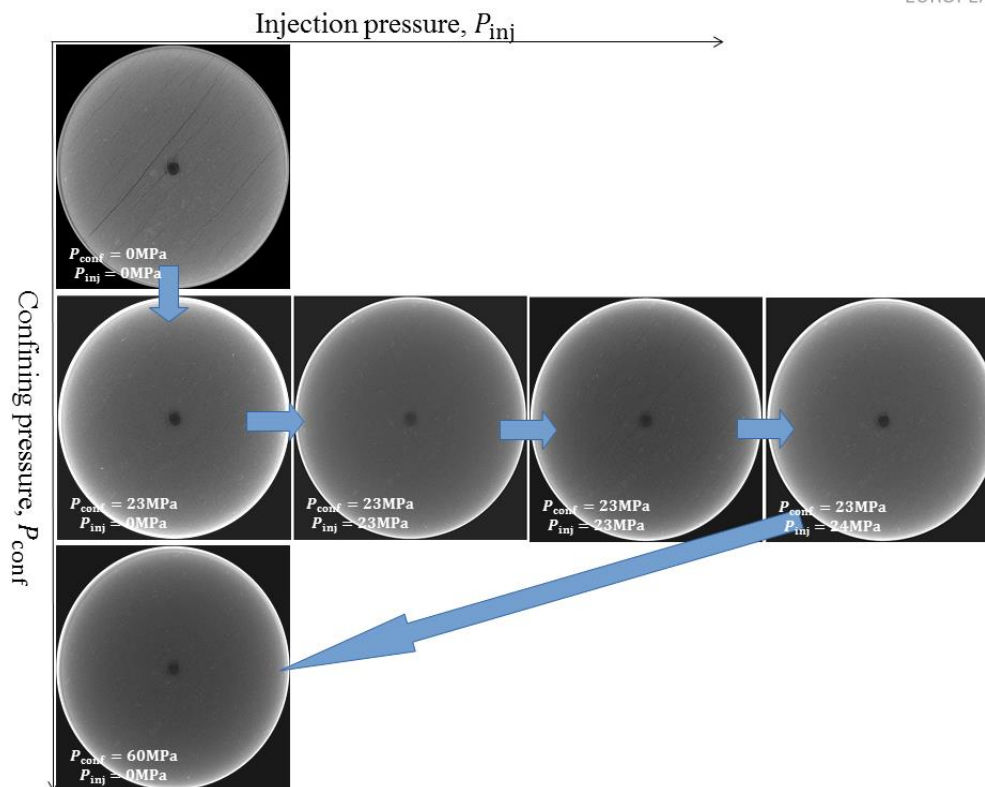


Figure 4: Tomograph cross-sections of a Haynesville shale sample cored parallel to bedding.

3.1.3 Next steps and social impacts

The team members will work on disseminating the knowledges acquired in this work package to industrial, local government and public to ensure people understanding the potential environmental impacts in shale gas industry.

Public perception has been identified as a major obstacle in shale gas development, but the majority of public are unfamiliar with it (Cooper et al., 2016). The team members will participate in public events, such as in library, museum and science in pub, to raise public awareness. Workshops with industry and governments will be held to make the knowledges useful for productions and policy-making.

3.1.4 Selected publications resulting from this work

- 1) Fauchille, A. L., Ma, L., Rutter, E., Chandler, M., Lee, P. D., & Taylor, K. G. (2017). An enhanced understanding of the Basinal Bowland shale in Lancashire (UK), through microtextural and mineralogical observations. *Marine and Petroleum Geology*, 86, 1374-1390.
- 2) Ma, L., Taylor, K. G., Dowey, P. J., Courtois, L., Gholinia, A., & Lee, P. D. (2017). Multi-scale 3D characterisation of porosity and organic matter in shales with variable TOC content and thermal maturity: Examples from the Lublin and Baltic Basins, Poland and Lithuania. *International Journal of Coal Geology*, 180, 100-112.
- 3) Fauchille, A. L., van den Eijnden, A. P., Ma, L., Chandler, M., Taylor, K. G., Madi, K., & Rutter, E. (2018). Variability in spatial distribution of mineral phases in the Lower Bowland Shale, UK, from the mm-to μm -scale: Quantitative characterization and modelling. *Marine and Petroleum Geology*, 92, 109-127.

- 4) Figueroa Pilz, F., Dowey, P. J., Fauchille, A. L., Courtois, L., Bay, B., Ma, L., & Lee, P. D. (2017). Synchrotron tomographic quantification of strain and fracture during simulated thermal maturation of an organic-rich shale, UK Kimmeridge Clay. *Journal of Geophysical Research: Solid Earth*, 122(4), 2553-2564.

3.1.5 References

Cooper, J., Stamford, L., Azapagic, A., 2016. Shale gas: a review of the economic, environmental, and social sustainability. *Energy Technology* 4, 772-792.

Figueroa Pilz, F., Dowey, P.J., Fauchille, A.L., Courtois, L., Bay, B., Ma, L., Taylor, K.G., Mecklenburgh, J., Lee, P.D., 2017. Synchrotron tomographic quantification of strain and fracture during simulated thermal maturation of an organic-rich shale, UK Kimmeridge Clay. *Journal of Geophysical Research: Solid Earth* 122, 2553-2564.

Fisher, M.K., Warpinski, N.R., 2012. Hydraulic-fracture-height growth: Real data. *Spe Prod Oper* 27, 8-19.

Rutter, E.H., Mecklenburgh, J., 2017. Hydraulic conductivity of bedding-parallel cracks in shale as a function of shear and normal stress. Geological Society, London, Special Publications 454, SP454. 459.

Thiercelin, M., Jeffrey, R., Naceur, K.B., 1987. The Influence of Fracture Toughness on the Geometry of Hydraulic Fractures, Low Permeability Reservoirs Symposium. Society of Petroleum Engineers.

3.2 Modelling of Confined Fluids

3.2.1 *Scientific questions addressed and environmental impacts addressed*

The properties of fluids when confined at the nanometre scale are significantly different from the properties of the correspondent macroscopic bulk fluid. Changes in phase behaviour, structural and transport properties are commonly observed under confinement. This is a consequence both of the small size of the system and of the interactions with the wall of the material confining the fluid.

Molecular simulations can be very useful in elucidating confinement effects and the underlying mechanism responsible for the observed behaviour. We employed classical Molecular Dynamics (MD) and Monte Carlo (MC) simulation techniques to study the structural and transport properties of two systems relevant to the shale gas upstream sector: (a) Water-based fracturing fluids confined in nano- and meso-pores of clay minerals (kaolinite, montmorillonite, muscovite) - major components of Bowland shale in the UK; (b) shale gas confined in mature type II kerogen (the insoluble part of organic matter found in shales that hosts the natural gas to be extracted). Results obtained from the simulations include preferential distribution in heterogeneous pores, diffusion coefficients, effects of fluid composition and porosity on diffusion coefficients of the fluid components.

Shale gas technology has been developed during the last three decades and it has been revealed that no two shales are the same. Therefore, the development of a shale formation into a productive reservoir requires customized design, through the adaptation and optimization of existing technologies. One of the major challenges faced by the industry is the rapid decay of production, which is associated with small recovery of the shale gas 'in place'. While hydraulic fracturing allows the recovery of an amount of gas that was originally inaccessible, the factors governing the transport of gas to the fractured clay matrix through the organic matter nanopores are still not well understood. The results of our molecular simulations will help to optimize and improve the extraction processes.

Currently, North America is the only major shale gas-producing region. This is partly attributed to environmental concerns associated with the extraction process in other parts of the world. Among other issues, there are concerns regarding the potential migration of naturally occurring radioactive materials (NORMs). The study of the NORM transport in confined fracturing fluid and their adsorption behaviour in the heterogeneous clay pores will help better understand and evaluate the environmental risks that could arise from shale gas operations.

3.2.2 *Main results achieved during the project*

3.2.2.1 *Water based fracturing fluids in clay mesopores*

New atomistic models of clays have been developed and used within the project: uncharged clay (**kaolinite**), lower-charge smectite (swelling clay, represented by **montmorillonite**), and

higher charge illite (non-swelling clay, represented by *muscovite*). For the first time, a significant attention is paid to the structure and adsorption of aqueous species at the non-basal edges surfaces of clay nano-particles.

For the adsorption on the basal surfaces of kaolinite, a slit type mesopore 40 Å wide was constructed by 4 kaolinite layers (each composed of a gibbsite and a siloxane sheet) created by a 9x9x4 arrangement of 324 crystallographic unit cells. In this way one gibbsite and one siloxane surfaces are exposed to the fracturing fluid on opposite sides of the pore. It was loaded with a model composition of a water based fracturing fluid - a mixture of water, a salt and an organic additive. For comparison reasons, simpler water solutions with either the salt or the additive were also considered. The salts examined were NaCl, CsCl, SrCl₂, and RaCl₂. Methanol and citric acid, both in its fully protonated and fully dissociated form, were the three model organic additives studied. Classical equilibrium MD techniques were used to simulate these systems. Preferential distribution of the various fluid components as function of their distance from the walls of the pore (along the z-axis) was calculated based on their atomic density profiles. The pore was divided into three regions (layers) based on the density profile of water and lateral diffusion coefficients along with residence times were calculated for each layer. The formation of citric acid aggregates and number of hydrogen bonds formed between the fluid species and the pore walls were also qualitatively analysed.

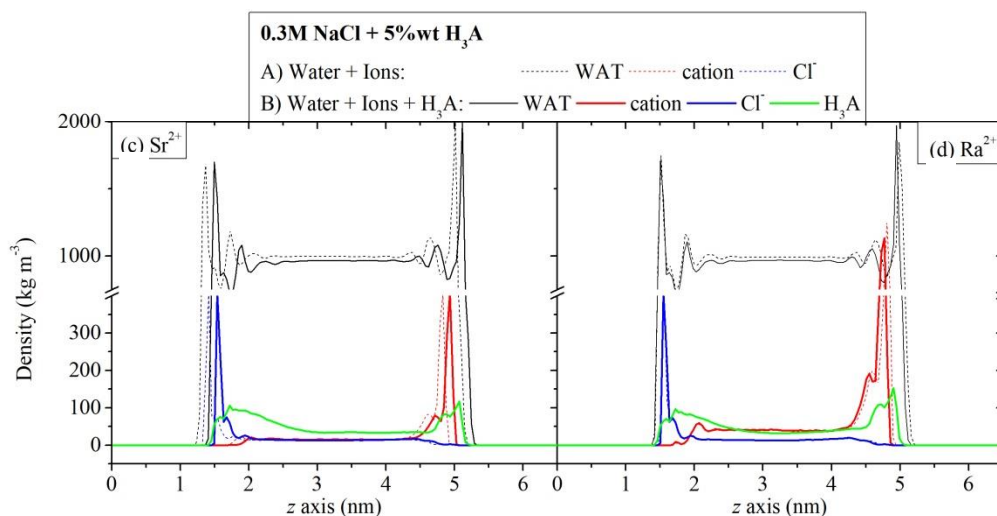


Figure 5: Atomic density profiles along the axis normal to the kaolinite (001) surfaces for the systems with and without the protonated citric acid (H₃A). a) NaCl, b) CsCl, c) SrCl₂ and d) RaCl₂. The RI and RIII regions of each diagram correspond to the gibbsite and siloxane surfaces, respectively.

Water density profile at kaolinite basal surfaces is generally symmetric with two peaks close to each wall. Cations prefer the siloxane side and anions the gibbsite side of the pore (**Figure 5**). Methanol and protonated citric acid are concentrated towards the siloxane pore wall, while the fully dissociated prefers the gibbsite side. Additives do not affect the density distribution of the ions and water. On the other hand, ions affect the distribution of citric acid. The addition of salt decreases the mobility of water, which is further decreased in the presence of additives. The effect of protonated citric acid is larger than the effect of

dissociated citric acid. Cation mobility ranking close to the siloxane surface is $\text{Na}^+ > \text{Cs}^+ > \text{Sr}^{2+} > \text{Ra}^{2+}$ with the reverse order characterizing their surface residence times. This ranking does not depend on the presence or the nature of the additive. Methanol mobility at the siloxane region remains unaffected by the salts. Protonated citric acid was found to have a higher residence time close to the siloxane surface compared to its dissociated form, while the opposite ordering is observed close to the gibbsite surface. It was also found that citric acid in its dissociated state tends to form a single large cluster while in the protonated state it forms smaller sized dynamically changing clusters.

At the (010) edge surfaces of montmorillonite in contact with Ba^{2+} and Sr^{2+} containing fluids, the atomic density profiles of H_2O molecules and ions (Figure 2) demonstrate quite a strong exchange between interfacial $\text{Ba}^{2+}/\text{Sr}^{2+}$ and interlayer Na^+ ions : $\sim 75\%$ of Ba^{2+} ions initially in the interfacial region enter the interlayers and remain contained there. This indicates that the divalent NORM cations, such as Ba^{2+} , Sr^{2+} , and Ra^{2+} , are preferentially distributed into the swelling clay interlayers, thus decreasing their ability to migrate to the surface during the fracturing process.

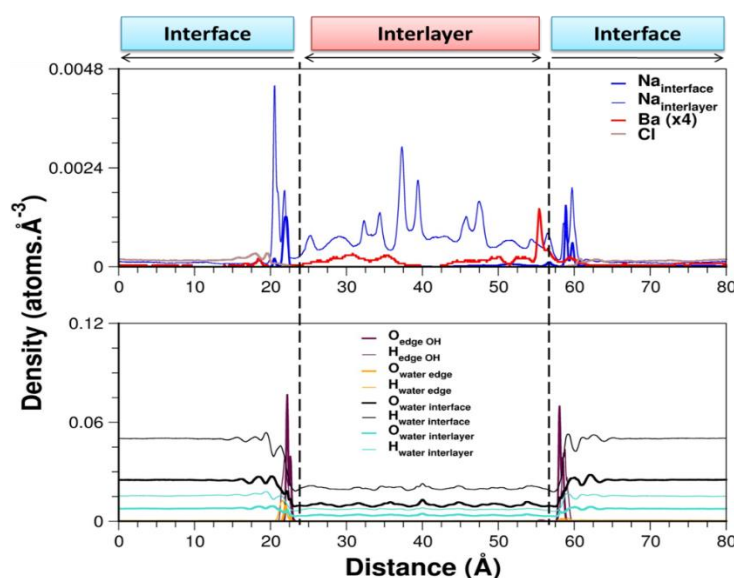


Figure 6: Atomic density profiles along the axis normal to the (010) montmorillonite surfaces for the systems containing 1480 H_2O molecules, 6 NaCl (0.1M), and 4 $\text{BaCl}_2/\text{SrCl}_2$ (0.07M).

Grand canonical Monte Carlo simulations were performed to predict **the solubility of NaCl in montmorillonite pores**, because the confinement is expected to affect not only the structure and dynamics of aqueous solutions, but also the solubility of electrolytes. The simulations were conducted at 365K and 275 bar. At these conditions, the simulation models implemented (SPC/E model for water Joung-Cheatham model for ions) predict saturation NaCl concentration in water of 3.14 mol/kg, which underestimates the experimental value of 6.1 mol/kg. We considered the pores of width ranging from 1.0 to 3.2 nm, and they were simulated in equilibrium with saturated bulk aqueous NaCl solutions. **Figure 7** shows the concentrations of the adsorbed ions in the nanopores are lower than in the bulk aqueous system, and decrease as the pore width narrows. We further compared

the aqueous solubility of NaCl in Na-montmorillonite and pyrophyllite pores of the same width. We were able to distinguish the ionic solubility near the center of the pore, where the properties are similar to those found in bulk water, and those near the pore surfaces, where the properties are significantly different compared to those found in bulk water. As the pore width decreases, the contribution of the region near to the pore surfaces increases compared to that of the fluids near the pore center, and as a consequence the NaCl solubility strongly decreases compared to that observed in bulk water.

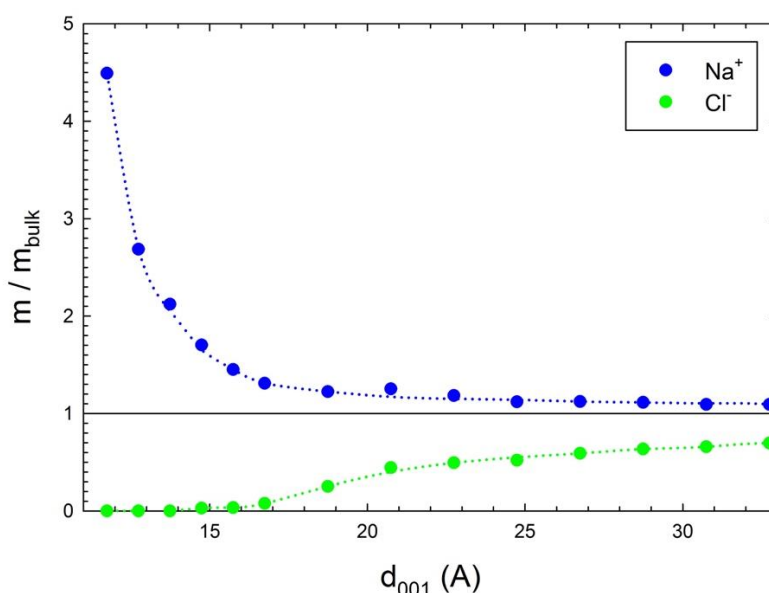


Figure 7: Ratios between confined and bulk concentration of Na⁺ and Cl⁻ electrolytes as a function of pore width.

3.2.2.2 Shale gas in type II kerogen

Transport properties of shale gas and its individual components were studied in 24 type II kerogen models comprising a variety of porosity characteristics (*e.g.* limiting pore diameter, accessible pore surface etc.). Shale gas was modelled as a mixture of methane, ethane, carbon dioxide and nitrogen having molar fractions of 0.85, 0.7, 0.4 and 0.4 respectively. The kerogen structures had been previously constructed using a well-established protocol based on isothermal isobaric (*NPT*) MD simulations. The porosity of the model structures was characterized with a newly developed algorithm, quantifying the number of pores in the structure, their degree of percolation, the maximum and limiting diameters, and the % porosity. The structures were loaded with the model gas by means of stochastic MC simulations at the grand canonical ensemble (GCMC) so that the confined gas is in equilibrium with the bulk gas phase at the same conditions. MD simulations were then performed at the canonical ensemble (*NVT*), and the self-diffusion coefficients of gas components calculated using the Einstein relationship from the slope of the molecular mean squared displacements versus time curve.

It was proven that ethane's diffusion coefficient is half the diffusion coefficient of methane, in every structure independently of its porosity characteristics. Limiting pore diameter is the

only porosity characteristic that has a strong effect on the observed diffusion coefficients, while the maximum pore diameter has no effect at all (**Figure 8**). There is also some dependence on the accessible surface area of the pore. A similar behaviour was observed for the other gases examined for both temperatures (298.15 K and 398.15 K) and pressures (1 atm and 250 atm) considered. A comparison of the transport properties of mixture components under confinement with their corresponding pure components values, showed that each component is not affected by the presence of other molecules in the mixture.

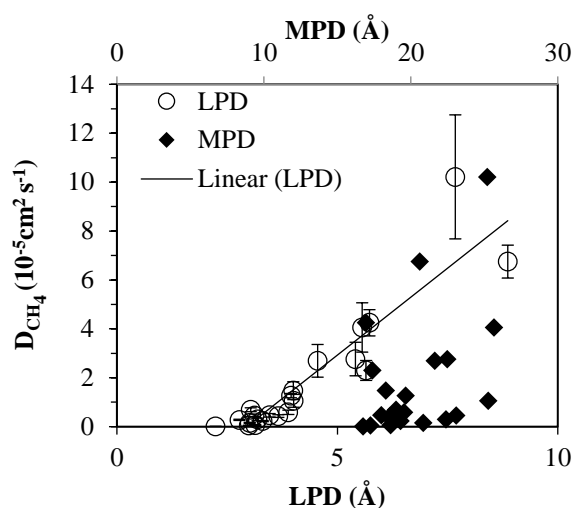


Figure 8: Maximum component of the diffusion coefficient of pure methane in a variety of type II kerogen models as function of the limiting (primary horizontal axis) and maximum (secondary horizontal axis) pore diameters of the structure at 298.15 K and 250 atm. A linear trend line is fitted to the D vs LPD points.

3.2.3 Next steps and social impacts

Improvement of the atomistic models of the pores typically found in shale formations (clays, kerogen, fluid compositions) is a promising direction for future research, possibly with the explicit inclusion of many body effects through polarizable models. The organic additives used in real fracturing fluids have much higher molecular weights and more complex molecular architectures, thus posing extra challenges for molecular simulation. Several approximations have also been made during the construction of the kerogen and clay models. It has been assumed a single molecule of relatively low molecular weight represents kerogen. Although these models are able to properly describe certain characteristics of the chemistry of the system and although they realistically describe porosity, the effect of the assumed kerogen molecular size, structure and model polydispersity on the observed properties needs to be investigated and quantified. Study of a wider variety of clays or hybrid pores composed of either different clay walls or kerogen/clay walls need to be investigated. Finally, a detailed study of the effects of pressure and temperature under confinement conditions is necessary in order to have a more complete understanding of these systems for hydraulic fracturing applications.

Optimization of the extraction process with simultaneous elimination of the environmental footprint to the upstream processes will have multiple benefits to the society. Accessibility

to all existing resources of shale gas will help to improve European energy sustainability of future generations. This will also have immediate benefits for the potentially productive regions by the creation of thousands of new jobs with subsequent economic benefits. Last but not least, apart from the fact that this will be conducted in an environmentally safe manner, the exploitation of shale gas resources will contribute to the decrease of GHG emissions. Shale gas is no different from conventional natural gas and shares all its advantages, including the limited GHG emissions compared to other fossil fuels, such as coal.

3.2.4 Selected publications resulting from this work

1) M. Vasileiadis, L.D. Peristeras, K.D. Papavasileiou and I.G. Economou, “Transport Properties of Shale Gas in Relation to Kerogen Porosity”, *J. Phys. Chem. C*, **122**(11), 6166 – 6177 (2018).

Abstract: Kerogen is a microporous amorphous solid, which is the major component of the organic matter scattered in the potentially lucrative shale formations hosting shale gas. A deeper understanding of the way kerogen porosity characteristics affect the transport properties of hosted gas is important for the optimal design of the extraction process. We employ molecular simulation techniques to investigate the role of porosity on the adsorption and transport behavior of shale gas in overmature type II kerogen found in many currently productive shales. Grand canonical Monte Carlo simulations were performed for the study of the adsorption of CH₄, C₂H₆, n-C₄H₁₀, and CO₂ at 298.15 and 398.15 K and a variety of pressures. The amount adsorbed is found to correlate linearly with the porosity of the kerogen. The diffusion of CH₄, C₂H₆, and CO₂, both as pure components and as components of the mixture, was investigated using equilibrium molecular dynamics simulations at temperatures of 298.15 and 398.15 K and pressures of 1 and 250 atm. In addition to the effect of temperature and pressure, the importance of limiting pore diameter (LPD), maximum pore diameter (MPD), accessible volume (V_{acc}), and accessible surface (S_{acc}) on the observed adsorbed amount and diffusion coefficient was revealed by qualitative relationships. The diffusion was found to be anisotropic and the maximum component of the diffusion coefficient to correlate linearly with LPD, indicating that the controlling step of the transport process is the crossing of the limiting pore region. The transport behavior of the pure compounds was compared with their transport properties in the mixture and it was found that the diffusion coefficient of each component is similar to the corresponding one under pure conditions. This observation agrees with earlier studies in different kerogen models comprising wider pores.

2) K.D. Papavasileiou, V.K. Michalis, L.D. Peristeras, M. Vasileiadis, A. Striolo and I.G. Economou, “Molecular Dynamics Simulation of Water-Based Fracturing Fluids in Kaolinite Slit Pores”, *J. Phys. Chem. C*, in press, July 2018.

Abstract: The adsorption behavior of aqueous salt solutions and additives inside kaolinite mesopores is investigated using Molecular Dynamics simulations. In particular, we examine the various combinations of water + salt, water + additive, and water + salt + additive mixtures, where the salts are NaCl, CsCl, SrCl₂ and RaCl₂ and the additives are methanol and citric acid (fully protonated, and fully deprotonated forms, with the latter being prevalent under neutral pH conditions). The atomic density distributions along the kaolinite pore reveal the preferential adsorption behavior of the various species with respect to the gibbsite and siloxane surfaces of kaolinite. Furthermore, we examine the hydrogen bonds formed between the kaolinite surfaces and water molecules as well as the additives. Citric acid tends to aggregate, and a cluster analysis examined the effect of various ions on the cluster formation. Finally, the calculated lateral diffusion coefficients and mean surface residence times provide insights on the mobility of the various species inside the kaolinite mesopores.

3) L. Michalec and M. Lísal, “Molecular simulation of shale gas adsorption onto overmature type II model kerogen with control microporosity”, *Molec. Phys.* **115**, 1086-1103 (2017).

Abstract: We use an all-atom molecular dynamics simulation to generate the dense porous structures of overmature type II kerogen with control microporosity. The structures mimic the organic part of Barnett shale under a typical reservoir condition of 365 K and 275 bar. Model kerogen structures were generated by gradual cooling and compression of the initial low-density random configurations of molecular kerogen units, using a dummy particle of varying size to introduce microporosity into the kerogen structures. The microporous kerogen structures were systematically characterized by calculating the geometric pore size distribution, pore limiting diameter, maximum pore size, accessible surface area, and pore volume and by analysing the pore network accessibility. Grand Canonical Monte Carlo (GCMC) simulation was employed to study the adsorption of two proxies of shale gas (pure methane and mixture of 82 % of methane, 12 % of ethane and 6 % of propane) in the kerogen structures. The shale gas adsorptions are compared with GCMC simulation of CO₂ adsorption in the kerogen structures. We complement the adsorption studies by exploring accessibility of kerogen pore space using molecular dynamics simulation. Finally, we introduce a mesoscale pore void into a microporous kerogen structure and probe the adsorption behaviour of the hydrocarbon mixture in such a multiscale kerogen model.

4) F. Moučka, M. Svoboda and M. Lísal, “Modelling aqueous solubility of sodium chloride in clays at thermodynamic conditions of hydraulic fracturing by molecular simulations”, *Phys. Chem. Chem. Phys.* **19**, 16586-16599 (2017).

Abstract: To address the high salinity of flow-back water during hydraulic fracturing, we have studied the equilibrium partitioning of NaCl and water between the bulk phase and clay pores. We use an advanced Grand Canonical Monte Carlo (GCMC) technique based on fractional exchanges of dissolved ions and H₂O molecules. We consider a typical shale gas reservoir condition of $T=365$ K and $P= 275$ bar, and represent clay pores by pyrophyllite and Na-montmorillonite slits of a width ranging from about 0.7 to 2.8 nm, covering clay pores

from dry clay to clay pores with a bulk-like layer in the middle of the pore. Adsorption of ions and water molecules in the clay pores is quantitatively evaluated and used to predict the salt solubility under confinement. Besides the thermodynamic properties, we evaluate the structure, in-plane surface diffusion of the adsorbed fluids, and ion conductivities.

5) A. Striolo and D.R. Cole, “*Understanding Shale Gas: Recent Progress and Remaining Challenges*”, *Energy and Fuels* **31**, 10300-10310 (2017).

Abstract: Because of a number of technological advancements, unconventional hydrocarbons, and in particular shale gas, have transformed the US economy. Much is being learned, as demonstrated by the reduced cost of extracting shale gas in the US over the past five years. However, a number of challenges still need to be addressed. Many of these challenges represent grand scientific and technological tasks, overcoming which will have a number of positive impacts, ranging from the reduction of the environmental footprint of shale gas production to improvements and leaps forward in diverse sectors, including chemicals manufacturing and catalytic transformations. This review addresses recent advancements in computational and experimental approaches, which led to improved understanding of, in particular, structure and transport of fluids, including hydrocarbons, electrolytes, water, and CO₂ in heterogeneous sub-surface rocks such as those typically found in shale formations. The narrative is concluded with a suggestion of a few research directions that, by synergistically combining computational and experimental advances, could allow us to overcome some of the hurdles that currently hinder the production of hydrocarbons from shale formations.

3.3 New Formulations to Reduce the Environmental Footprint

3.3.1 *Scientific questions and environmental impacts addressed*

The main task of WP5 is the formulation of hydraulic fracturing fluids specific for the shale formations found in Europe. Since every shale formation is unique, fracturing fluids effective in North American shale formations might not be effective in European ones. In this framework the study of formulations with physico-chemical properties that are appropriate with the pressure-temperature conditions and the composition of shale gas formations is fundamental for the potential exploitation of European shale basins.

At the same time, environmental concerns about shale gas extraction cast doubts on the toxicity of the chemicals which are present in fracturing fluids. To minimize the environmental impact of hydraulic fracturing and reduce the amount of pollutants in flowback and produced water, all the substances which are potentially dangerous are replaced by greener alternatives. On this basis, the four primary objectives of WP5 are:

- 1) To formulate effective hydraulic fracturing fluids that contain no hazardous substances;
- 2) To formulate hydraulic fracturing fluids that are effective at high salt concentrations;
- 3) To generate a scientific method for the formulation of fluids based on the geochemical properties of a shale formation;
- 4) To design additives that limit the extraction of salt and NORM from shale formations.

By following the abovementioned guidelines, we worked on alternative and innovative fracturing fluid formulations that significantly reduce the environmental footprint related to the shale gas extraction, especially from the perspective of the environment and groundwater (and consequently aqueducts) chemical contamination.

3.3.1.1 Where we started from: the existing formulations

There are several types of fracturing fluids, but in most cases the formulations are composed by: base fluid, proppant, and additives [1]. Water-based fluids are applied in approximately 80% of the wells and they can use as water source fresh water, seawater, brine, or a saturated brine, depending on the well conditions or on the drilled interval of the well [2,3]. The compounds added to the frac-fluids fulfil three main functions: enhance the fluid performances, improve the capability to carry the proppant and minimize formation damage [4]. The additives commonly used include: thickening agents, crosslinking agents, temperature stabilizers, pH-control agents, gel breakers, scale inhibitors, corrosion inhibitors, biocides, and surfactants.

In order to formulate green and environmentally friendly frac-fluids, we pursued two different strategies: one based on biopolymers and another one on viscoelastic surfactants. More precisely, we investigated Guar Gum (GG), Sodium Hyaluronate (SH) and HydroxyPropyl Cellulose (HPC) as polysaccharides. These fluids were tested in model solvent (pure water) and in the presence of high amount of salt. We investigated the effect of both salt concentration and nature on the formulation properties. Then we studied specific additives like surfactants in

order to optimize the multifunctional performances of the formulation. Simultaneously, we also explored as multifunctional components for unconventional fracturing fluids two ViscoElastic Surfactant (VES) systems, one based on Sodium Oleate (NaOL) plus KCL and the second one based on cetyltrimethylammonium bromide (CTAB) combined with sodium salicylate (NaSal).

The proposed formulations are designed to cover a wide range of viscosities and rheological behaviours, thus ensuring their applicability in various basins characterized by different rock composition and where different fluid properties may be required.

3.3.2 Main results achieved during the project

3.3.2.1 Polysaccharide-based Formulations

In order to check the effectiveness of our formulations at high-salinity conditions we tested different salt solutions, by following three complementary approaches.

At first, we collected the responses of our formulations to a set of thirteen different salts/co-solute, in the individual concentration of 0.5 mol/L. The salts/co-solutes examined are urea ($\text{CH}_4\text{N}_2\text{O}$), trehalose ($\text{C}_{12}\text{H}_{22}\text{O}_{11}$), potassium chloride (KCl) and ten sodium salts (NaF, NaCl, NaBr, NaI, Na_2SO_4 , NaSCN, NaClO_4 , Na_3PO_4 , Na_2HPO_4 , NaH_2PO_4). As can be seen in **Figure 9**, various salt/co-solute can have a strong effect on the rheological properties of the formulations, even leading to a remarkable change in viscosity. These results confirm how the presence of specific salts can strongly affect the robustness of the network and, consequently, represent a potential trigger to control and modify the fluid viscosity. So, starting from the knowledge of the salt composition and concentration of each different shale basin, we can choose the better formulation that fits with the required operative conditions.

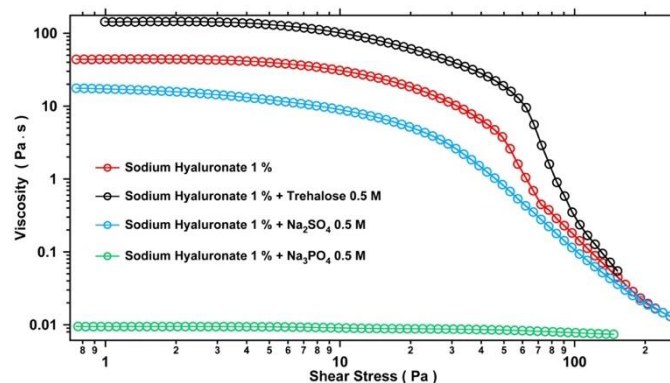


Figure 9: Influence of some specific salts on Sodium Hyaluronate viscosity.

Secondly, we tested our formulations in a mixed salt solution that we called “shale water” (SW). To prepare SW we took into account data available for the flowback water salinity content of some European shale basins [5,6]. Shale water is composed by NaCl 1 M, CaCl_2 0.2 M, KBr 0.014 M, SrCl_2 0.01M and BaCl_2 0.002 M. The assumption underpinning these experiments is that the salt composition and concentration of the flowback water should be not too dissimilar from the salinity conditions present downhole. Thus, by examining our formulations in shale water we

are able to qualitatively predict how these fluids behave in salinity conditions near to the operating ones. As shown in **Figure 10**, both the GG and SH based formulations exhibit good salt tolerance and their rheological profile is only slightly affected; in the case of HPC the high salinity conditions strengthen the network and increase the viscosity. However, all the investigated systems show a good resistance towards high salinity environment.

Finally, we performed additional tests aimed at qualitatively detect the salt toleration thresholds of the various formulations. For reaching this goal we overstressed the salt concentration up to 5 mol/L, a much higher value in comparison with the averaged total salinity of European flowback water. Since sodium chloride is commonly the most abundant salt present in the flowback water, we carried out our experiments by simply varying the concentration of NaCl from 0.1 to 5 M. Even in these overstressed conditions, the three polysaccharides exhibit behaviours analogous to those observed in shale water.

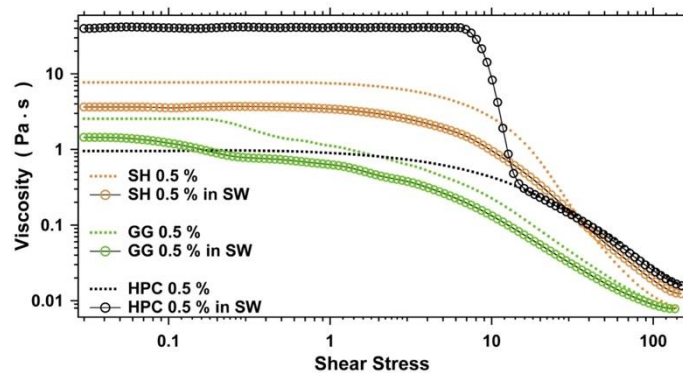


Figure 10: Rheological behaviours of Guar Gum, Sodium Hyaluronate and HydroxypPropyl Cellulose both in water and in high salinity conditions (Shale Water).

With the purpose of further enhancing the salt tolerance of our formulations, and always looking towards a more complete and functional fluid, we evaluated the addition of green surfactants/additives effective in enforcing the network and helping to efficiently carry the proppant. We added once at time and in extremely small content, equal to 0.05 % in weight, saponin, rhamnolipid and sodium citrate. In detail, we observed that both saponin and sodium citrate play a constructive role in the formation of the polysaccharide network (see **Figure 11**), especially if combined with HPC and GG; whereas, rhamnolipid weakens the structure and lowers move the viscosity, specifically those of SH and GG.

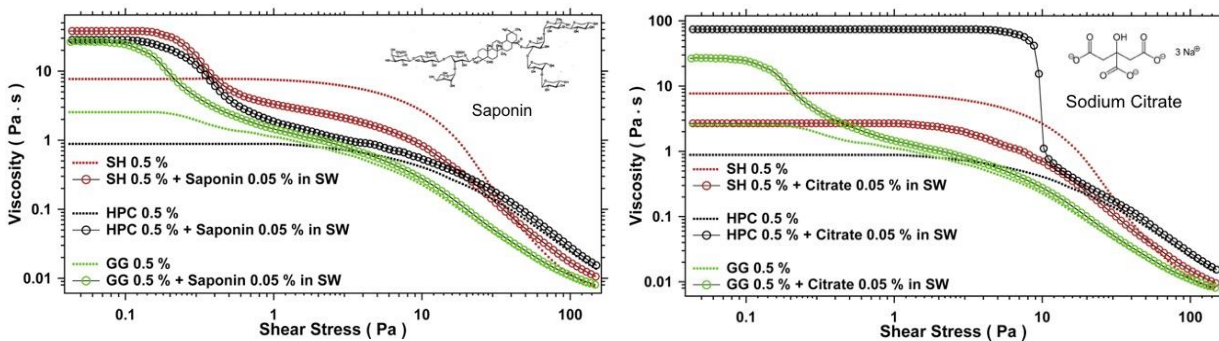


Figure 11: on the left, flow curves of GG, HPC and SH in water and in the simultaneous presence of SW and saponin; on the right, flow curves of GG, HPC and SH in water and in the simultaneous presence of SW and sodium citrate.

Moreover, we evaluated the addition of green anti-scale agents, such as polyglutamate and polyaspartate, able to replace the hazardous and commonly used polyacrylate. In order to test the effectiveness of these compounds, a small amount (0.001% w./w.) of the anti-scale agent is added to the formulation and, successively, the precipitation of the naturally most abundant scales (CaSO_4 , SrSO_4 , CaCO_3 and BaSO_4) is observed. Afterwards, the precipitated crystals are examined by optical microscopy imaging in order to check how their growth is influenced by the different anti-scale. **Figure 12** shows the precipitation carried out of CaSO_4 in the SH formulation. All the anti-scale additives astonishingly reduce the precipitation of the salt. This result means that the green and non-toxic alternative anti-scale agents could well replace the actually used polyacrylate. Moreover, by focusing on the microscopy images it is possible to notice that the green additives lead to the precipitation of smaller scales in comparison with the polyacrylate and, consequently, they contribute to preventing pipe obstructions. The tested anti-scale agents are effective in reducing the precipitation of both calcium and strontium salts, whereas they do not show significant effect on barium.

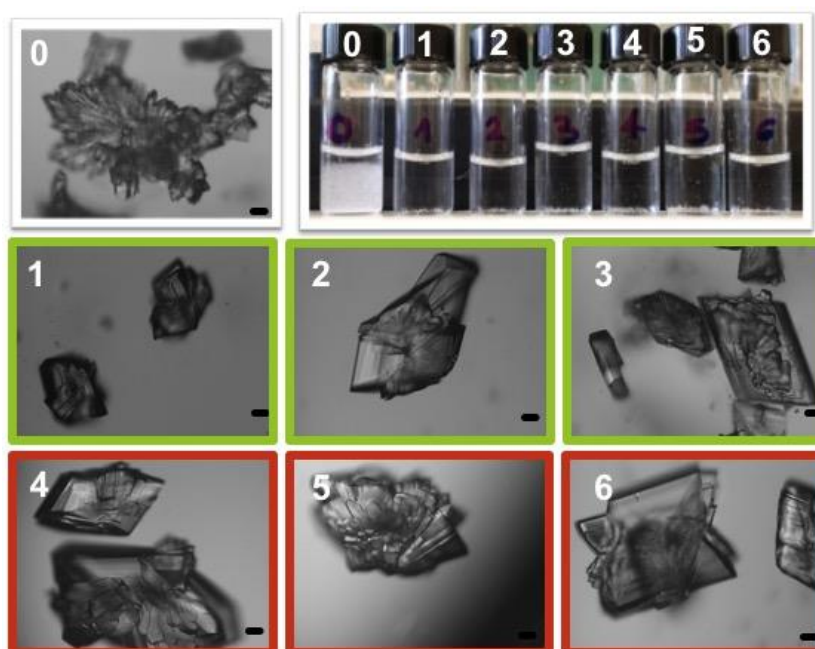


Figure 12: Precipitation of CaSO_4 in SH formulation. The numbers from 0 to 6 indicate the different anti-scale agent added: 0-no anti-scale agent, 1-polyaspartate, 2-low molecular weight polyglutamate, 3-high molecular weight polyglutamate, 4-low molecular weight polyacrylate, 5-intermediate molecular weight polyacrylate, and 6-high molecular weight polyacrylate. All the scale bars are 100 μm .

3.3.2.2 ViscoElastic Surfactant (VES) – based formulations

The two investigated water-based viscoelastic surfactant (VES) formulations contain a surfactant as the main component in combination with an inorganic salt or a charged molecule. The surfactants selected form long elongated micellar structures, capable of contributing to the viscoelastic behaviour and increasing fluid viscosity [7]. **Figure 13** shows how, by selecting the appropriate surfactant/salt ratio, rheological properties of the VES formulation are easy-tunable and matchable for the specific basins. Moreover, the NaOL+KCl formulation shows a singular behaviour when high pressure is applied to the system. Indeed, contrary to what

observed for the polysaccharide systems, the higher the applied pressure to the NaOL formulation the higher the viscosity exhibited (see **Figure 13** bottom). Other peculiar features of this VES system are the fast capacity of recovery after the application of a stress and the low resistance towards the thermal stress, which in turn requires specific additives.

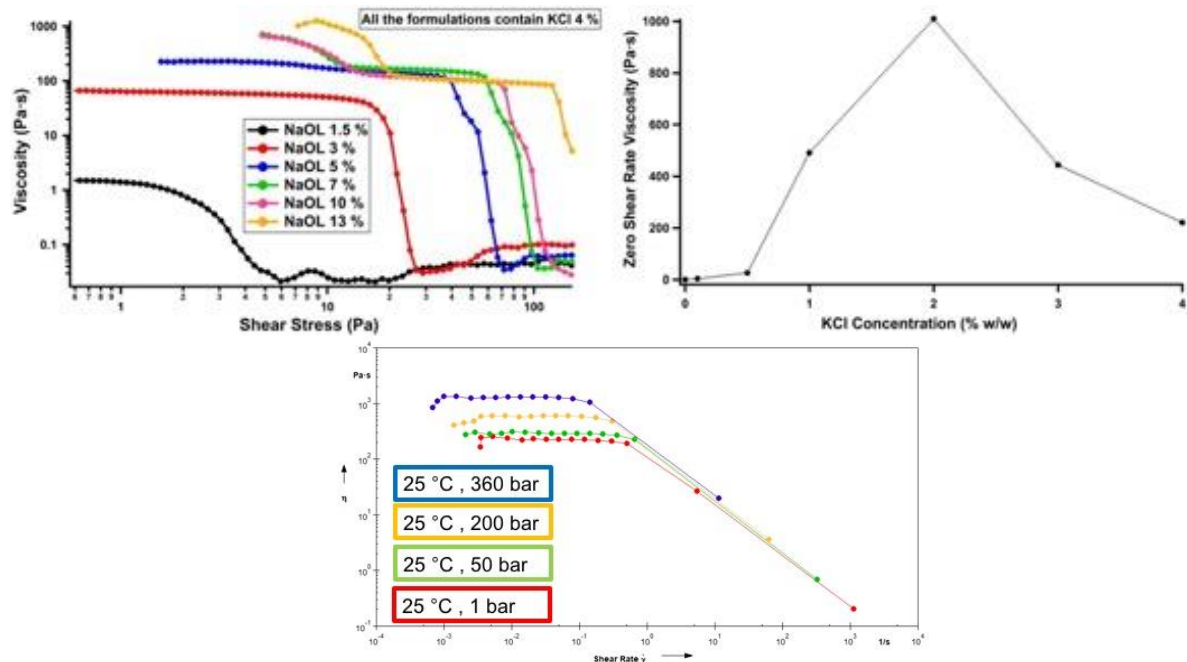


Figure 13: on the left, flow curves of VES formulations at different sodium oleate (NaOL) concentration and fixed KCl content; on the right, zero-shear viscosities of 13% w. NaOL at various KCl concentrations; bottom, flow curves acquired on NaOL 13% w. + KCl 4% w. at different applied pressures.

3.3.2.3 *“Smart” Responsive Formulations*

The formulation of “smart” frac-fluids responsive to both electric and light stimulation is obtained by the inclusion in the polysaccharide/VES matrix of specific additives. More specifically, to impart electro-responsiveness to both the polysaccharide and NaOL systems carbon black (CB) is added, while to make NaOL formulation light-responsive the food dye azorubine (AZO) is introduced in the micellar network.

As it is shown in **Figure 14**, by the addition of carbon both the viscosity and the thermal resistance of all the systems, both polysaccharides and NAOL/KCl, are enhanced. Moreover, the presence of CB induces electro-responsiveness in the HPC and SH formulations, which exhibit a separation in two distinctive phases, characterized by different rheological properties, after the application of a difference of potential of 30 V for one hour (**Figure 14** bottom left). The same electrical treatment works also on the NaOL formulation, leading in this case in an overall strengthen of the micellar network without a phase separation (**Figure 14** bottom right). Thus, CB could represent the key-additive to control the viscosity by the application of a voltage.

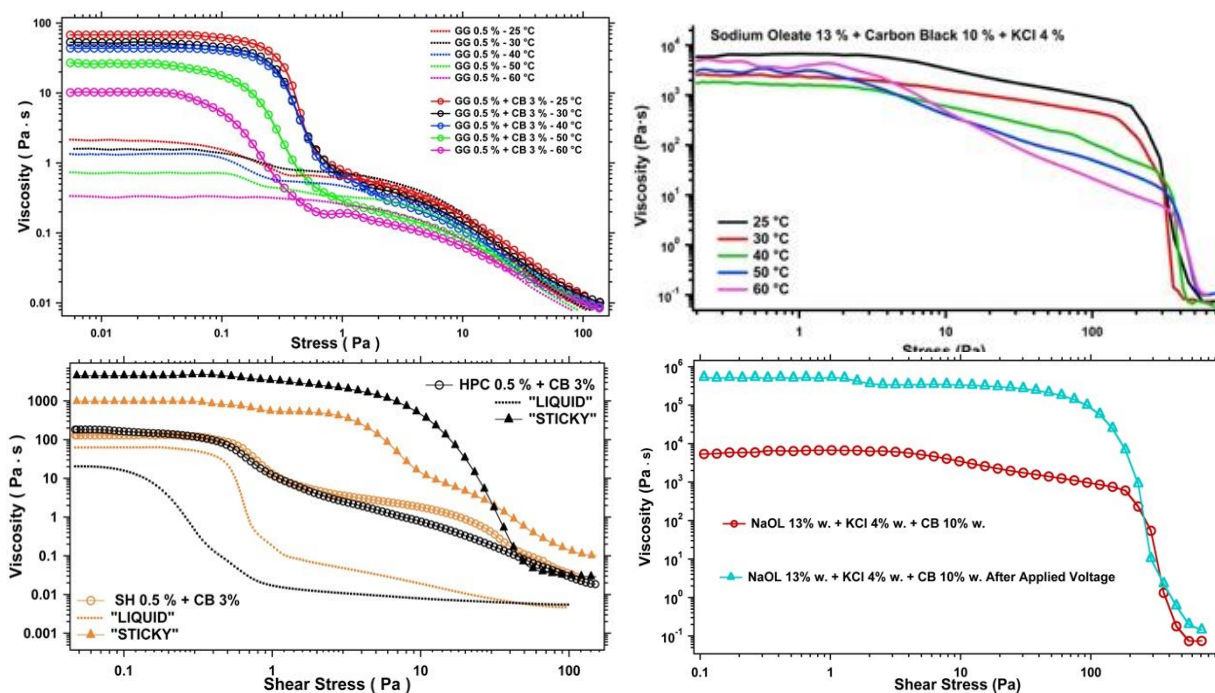


Figure 14: on the top left, flow curves of GG formulation, both with and without the addition of CB, acquired at different temperatures ranging from 25 °C to 60 °C; on the top right, flow curves of NaOL + CB formulation acquired at different temperatures ranging from 25 °C to 60 °C; on the bottom left, flow curves of SH + CB and HPC + CB formulations acquired both previous and after the electrical treatment; on the bottom right, flow curves of NaOL + CB formulation acquired both previous and after the electrical treatment.

By adding the red dye azorubine, which is approved by the food, drug and cosmetics (E122),[8] to the NaOL/KCl system is it possible to obtain a photo-responsive to the UV irradiation. When irradiated with UV light the Azorubine molecule undergoes a trans-cis isomerization changing its steric hindrance and, consequently, affecting the entanglement of the micelles and the rheological properties of the fluid (**Figure 15**). Azorubine allows to modulate the rheological properties through UV irradiation (achievable with an optical fibre) resulting in a two order-increased viscosity and a reduced critical stress needed to obtain the easy flow of the fluid.

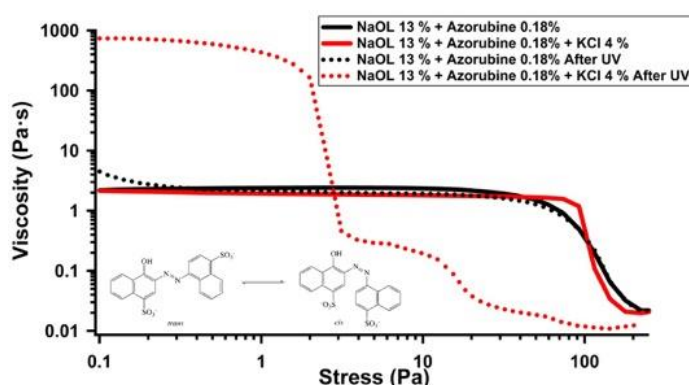


Figure 15: flow curves acquired on NaOL/KCl formulations, both with and without the addition of azorubine. Continuous and dotted lines represent non-irradiated and irradiated samples, respectively.

3.3.2.4 NORM reduction strategies

To reduce the amount of the *naturally occurring radioactive materials* (NORM) in flowback water, or at least facilitate their treatment, we pursued two parallel strategies: one based on the addition of anti-scale agents and a second one that exploit the effect of magnetic field on the precipitation of salts that contain radioactive isotopes.

By effectively reducing the precipitation of scale like SrSO_4 , which contain one of the most abundant NORM like Sr^{2+} , anti-scale agents contribute to reduce NORM concentration in the flow-back water, in addition to the prevention of pipes obstruction.

The second strategy is based on the application of a magnetic field (≈ 0.4 T) combined with a temperature of 60°C . The precipitation of the most abundant scales begins at this temperature, which is reached by the fluid at a certain depth in the vertical section of the different the wells. The simultaneous effect of magnetic field and medium-high temperature leads to an overall reduction of the precipitated scales and a reduction in their sizes, as it is shown in **Figure 16**.

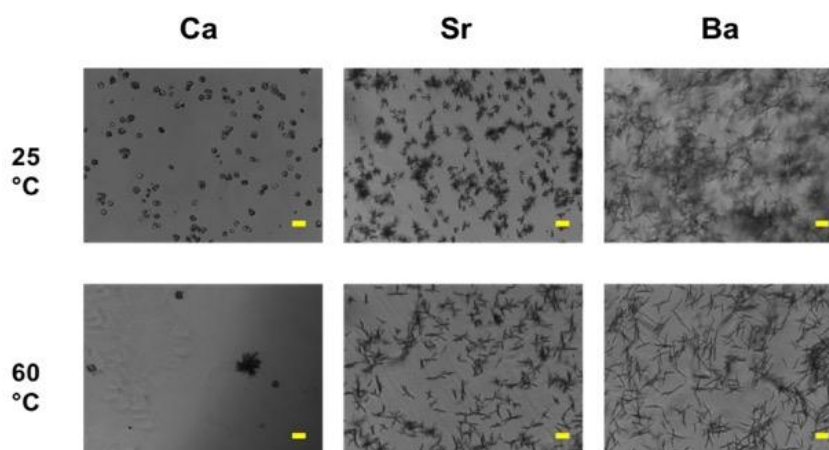


Figure 16: Optical microscopy images about the precipitation of CaCO_3 , SrCO_3 and BaCO_3 when a magnetic field of ≈ 0.4 T is applied at 25°C (top) and at 60°C (bottom). All the scale bars are $100\ \mu\text{m}$.

3.3.3 *Next steps and social impacts*

From the perspective of energy sources, shale gas could play a crucial role in the next future of Europe because it “can be a possible substitute for more carbon intensive fossil fuels, an indigenous source of natural gas reducing dependency on non-EU energy suppliers” [9]. However, a safe and environmentally sound development of this process is necessary in order to manage this energy by minimizing any undesired side-effects. Along these lines, our research was planned and carried out in order to design green and innovative frac-fluids able to reduce the environmental footprint by using only environmentally-friendly compounds for the extraction of the shale gas from European formations.

The achieved scientific findings could turn in a benefit for both the society and the environment, especially from the perspective of a reduced chemical contamination of the soil and the groundwater. Moreover, the use of green and friendly compounds in the formulation of frac-fluid helps to improve the perception and the image in the eyes of the public opinion. A

clear and transparent communication can be the key to bring people closer and make them more familiar with this energy source and the procedures related to its extraction. For these reasons it is important to carry on the research with the aims of improving the different fluid formulations, with the replacement of other additive with their green alternatives (*i.e.* antimicrobial agents, crosslinkers, corrosion control agents, etc.), of further reducing the NORM extraction, and of designing new formulations able to cover a wider range of properties and match with a broader types of rock formations.

3.3.4 Selected publications resulting from this work

Tatini, D., Sarri, F., Maltoni, P., Ambrosi, M., Carretti, E., Ninham, B. W., & Lo Nostro, P. (2017). Specific ion effects in polysaccharide dispersions. *Carbohydrate Polymers*, 173, 344–352.

Raudino, M., Sarri, F., Tatini, D. Ambrosi, M., Aloisi, G. D., Ninham, B. W., Dei, L., & Lo Nostro, P. (2108). The effect of temperature and magnetic field on the precipitation of insoluble salts of alkaline earth metals. *Just submitted*

Raudino, M., Sarri, F., Tatini, D. Ambrosi, M., Aloisi, G. D., Ninham, B. W., Dei, L., & Lo Nostro, P. (2108). Carbon black induces electrical responsiveness in green biopolymers and viscoelastic formulations. *Just submitted*

Tatini, D., Sarri, F., Delle Vaglie, A., Raudino, M., Ambrosi, M., Carretti, E., Ninham, B. W., & Lo Nostro, P. (2018). Light-modulated rheological properties of innovative formulations. *Just submitted*

3.3.5 References

1. <http://www.shale-gas-information-platform.org>
2. Gidley, J.L., Holditch, S.A., Nierode, D.E. et al. 1989. *Fracturing Fluids and Additives*. In *Recent Advances in Hydraulic Fracturing*, 12. Chap. 7, 131. Richardson, Texas: Monograph Series, SPE.
3. http://petrowiki.org/Drilling_fluid_types
4. Harris, P. C. (1988). *Fracturing-Fluid Additives*. *Journal of Petroleum Technology*, 40(10), 1.277-1.279.
5. Michel, M. M., & Reczek, L. (2014). *Pre-treatment of Flowback Water to Desalination*. *Membranes and Membrane Processes in Environmental Protection Monographs of the Environmental Engineering Committee Polish Academy of Sciences*, 119, 309–321.
6. Jiang, Q., Rentschler, J., Perrone, R., & Liu, L. (2013). *Application of ceramic membrane and ion-exchange for the treatment of the flowback water from Marcellus shale gas production*. *Journal of Membrane Science*, 431, 55–61.
7. Thampi, N. V., John, R. P., Ojha, K., & Nair, U. G. (2016). *Effect of Salts, Alkali, and Temperature on the Properties of Sodium Oleate Hydrogel*. *Industrial & Engineering Chemistry Research*, 55(20), 5805–5816.

8. König, J., in *Colour Addit. Foods Beverages* (Edited by M.J. Scotter), Woodhead Publishing, Oxford, 2015, pp. 35–60.
9. Communication from the commission to the council and the European parliament on the exploration and production of hydrocarbons (such as shale gas) using high volume hydraulic fracturing in the EU. Brussels 22.01.2014.

3.4 Analytical Models and Software

3.4.1 *Scientific questions and environmental impacts addressed*

Transport of fluids within rock mass, which is solid rock matter plus discontinuities such as fractures or faults, is a scale-dependent phenomenon. On the small scale (micro-scale), which is within intact rock, transport is through pores and micro-fractures. Above a certain scale (on the meso-scale), which is in general in the decimetre range, persistent discontinuities are evident; these discontinuities may be layering in sedimentary rocks, such as shale, and fractures. The fractures are typically evident in distinct orientations, which is the result of geological processes at geological time scales (millions of years). Commonly, the fractures are connected and make up the so-called distinct fracture network (dfn). Transport is governed by these fractures on the meso-scale.

At larger scale, decametre and above, faults are evident. Faults are large scale discontinuities, that show high fracture densities. These faults may be conductive in certain cases but may also be smeared and impermeable due to diagenetic processes or large deformation. Non-conductive faults confine oil- and gas-bearing compartments.

These general statements are valid for shale formations also. Pores contribute to fluid transport on the sub-centimetre scale, at larger rock volumes fractures increasingly become the dominant fluid transport pathway. Faults may be hydraulically confining reservoirs and act as fluid transport barriers. For a broader introduction to the matter, the reader is referred to Grotzinger and Jordan (2017).

WP6 was tasked with establishing a connection between atomistic, molecular-scale calculations and predictions for large-scale transport of fluids within shale rock formations. With this it is possible to use laboratory measurements of rock and predict (upscale) permeability for large scale applications. With this, it is possible to analyse the environmental impact of any shale gas exploration or production much better. Examples are the simulation of fluid migration in fracture networks and faults, or the assessment of the risk for induced seismicity.

The work summarised focusses on using micro-scale modelling and permeability measurements to study the influence of fractures on the transport of fluid in shale rock mass. Modelling of a typical shale play fracture network has been conducted and simulation of fluid transport with increasing model size has been conducted to identify a so-called representative elementary volume for bulk permeability. This bulk permeability tensor, which is dependent on the rock permeability and the distinct fracture network appearance, may be used within reservoir scale simulations to analyse fluid transport on the large scale.

The primary objectives are:

- The incorporation of shale rock permeability measurements and analytical model validation into meso-scale simulations of fluid transport in shale rock mass;
- The development of a workflow to upscale bulk permeability for macro-scale reservoir simulations;
- Conduction of macro-scale simulation of a generic to show the feasibility of the approach in simulation of fluid distribution and production within shale plays.

3.4.2 Main results achieved during the project

3.4.2.1 Microscopic transport modelling

SXT developed a lattice-based kinetic Monte Carlo (KMC) model to study fluid transport through slit-shaped pores with different chemical composition. The substrates analysed represent the main components of the inorganic material found in shale rocks. The proposed stochastic model was validated against the analytical solution of the diffusion equation and molecular dynamics (MD) simulations on slit pores. It was found that the chemistry of the pores affects the transport behaviour of methane molecules, as reported in previous studies. The hydrated silica nanopores exhibit the highest permeability, followed by the permeability observed in hydrated magnesium and alumina pores. The agreement between the KMC model and MD simulations is quantitative, however, the computational times are significantly reduced when using the KMC model.

The model was then extended in 2-dimensions and was used to provide insights regarding the contribution of the pore network characteristics in the transport behaviour. Two deterministic methods were also used for these investigations. Based on our analysis, among the three approaches considered here the KMC method is considered to be the most sensitive and reliable method. This method responds to changes in both the low and high permeability values. The most valuable feature of the KMC method, compared to the deterministic methods considered, was its sensitivity to anisotropy. For broad distributions, the EMT always over-estimated the network's permeability, the Simplified Renormalisation method provided low estimates, due to the zero cross-flow assumption, while the KMC predictions were in-between the two. Our model can be considered as a bottom-up approach for mesoscopic studies. Any type of designed or natural network can be simulated, as long as the kinetic (diffusion constants) and thermodynamic (barriers due to the interfaces) properties are provided.

The KMC approach as developed by SXT responds to changes in both the low and high permeability values. For dual-permeability networks, KMC detected changes proportional to the components and provided an estimate that captured the matrix structural features. The most valuable feature of the KMC method, compared to the deterministic methods considered, was its sensitivity to anisotropy. KMC could be applied to low-connectivity networks and could also quantify the effect of small-scale heterogeneities (*e.g.*, local low connectivity). When KMC was applied to predict the permeability of a shale sample for

which one SEM image was available together with data on pore-size distributions, the results obtained were reasonably close to experimental data, when considering the organic matter to be the highly permeable portion of the matrix. The method’s accuracy can be improved by extending our analysis to more images of a plug sample, so anisotropy and local heterogeneities are considered, accounting for the effect of adsorption and the true porosity. The disadvantage of the KMC method, compared to deterministic techniques, rests with the computing time required. The deterministic methods provided results in a few seconds, while the computational cost of KMC ranged from minutes to hours. Therefore, a future challenge is to efficiently use the KMC method to analyse permeability of a whole plug sample, while accounting for realistic phenomena such as preferential adsorption.

The implementation of the approach requires experimental information such as imaging of the rock samples, adsorption measurements for estimating the pore size distribution, and chemical composition analysis. Experimental information such as permeability can then be used to validate the approach proposed here.

3.4.2.2 Geomechanical modelling and permeability simulation

For the Whitby Mudstone (Boersma 2016) a upscaling simulation workflow was developed. The simulation has been performed using the research and development software package roxol™ (www.roxol.de), which is based on the eXtended Finite Element Method (XFEM). Based on statistical data, which was used to generate statistical distinct fracture networks by means of a newly developed fracture network generator for roxol of increasing size, the resulting bulk permeability of the domains was analysed. As can be seen in **Figure 17**, permeability increases with model area approaching asymptotically constant values for the permeability tensor. This bulk permeability of the representative elementary volume may be considered as bulk rock mass permeability as needed for large scale reservoir engineering and geomechanical simulations.

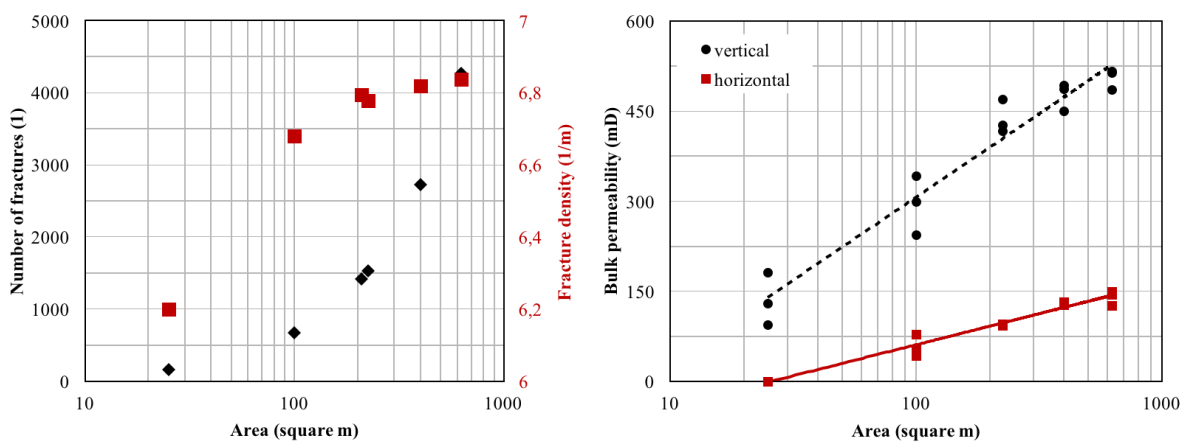


Figure 17: Increasing number of fractures and fracture density with increasing area (left) and increasing bulk permeability with increasing investigated scale following a logarithmic law for vertical and horizontal flow (right).

3.4.2.3 Simulation of fracture network evolution by hydraulic stimulation

To gain an understanding about the change in rock mass during hydraulic stimulation, a series of fracture mechanics numerical simulations was performed.

To quantify the change in permeability, the distinct fracture network was subject to an injection pressure into a central fracture. The fracture network extended by fracture propagation and coalescence. **Figure 18** shows examples of the fracture network evolution.

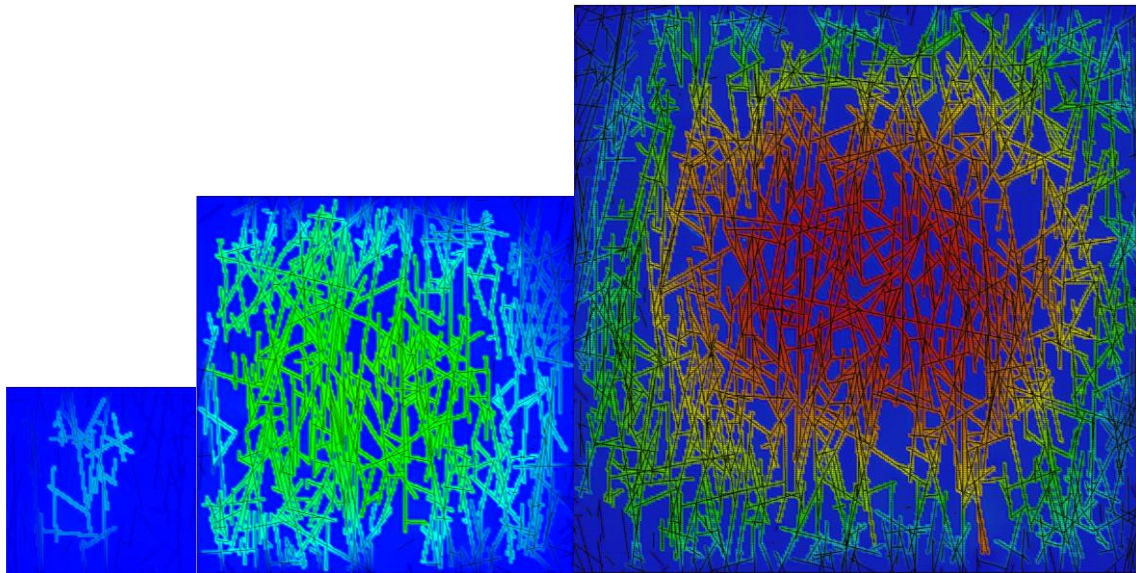


Figure 18: Fracture network extension examples. The fracture domains are 5x5, 10x10 and 15x15m and depicted in relative scale. The colour code indicates fluid overpressure in fractures, blue: 0 MPa and red: 11 MPa.

The evolution of the fracture network was not confined to a small zone of interconnecting fractures, but a distinct volume was altered, as is to be expected in fractured rock mass like in shales. This alteration of the fracture network also yields changed permeability.

The permeability of the stimulated fracture network was determined with the workflow described previously. An increase of permeability could be shown which is solely mechanically introduced; fracture healing or chemical effects are not considered here. Permeability was increased by a factor of about 1.5.

To understand how far fracture coalescence would reach into the formation, a series of simulations in beams with and without pre-inscribed fracture networks was carried out. It could be clearly seen in these fracture mechanics simulations with roxol, that at constant injection pressure the fracture network would be changed along with the permeability of the rock mass, but that at some point fracture propagation would ease and a stable fracture network establishes. For typical shale injection pressures, the radius of impact is in the order of some decametres.

3.4.2.4 Reservoir scale analysis

Analysis of geomechanical reservoir performance may be done using the derived permeability characteristics of shale reservoirs. In the following a workflow is outlined, that shows how the parameters may be used on the example of induced seismicity.

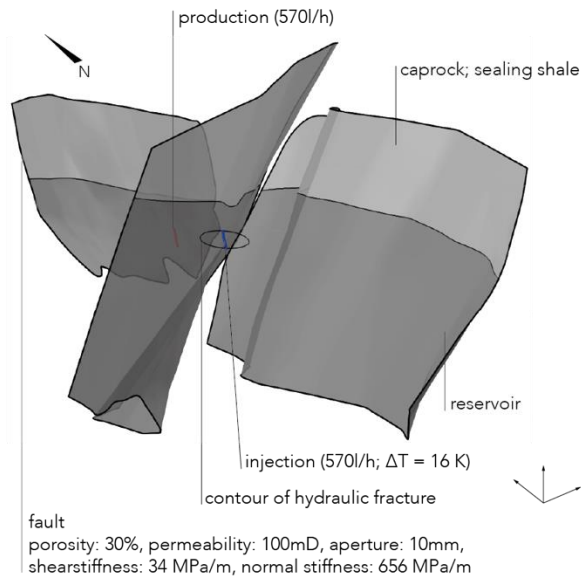
Induced seismicity has become a topic of major awareness not only in the hydrocarbon or geothermal industry, but in public as well. The reason for the growing interest is manifold. While the public is mainly concerned about safety, the interest in the fluid mining industry on induced seismicity additionally stems from the wish to monitor changes in the reservoir performance (Zoback 2010), observe stress changes on faults (King et al. 1994), or to estimate the extent of hydraulic fracturing campaigns (Shapiro 2015). Induced seismicity has also been used to optimise the fluid injection rates of geothermal power plants or to avoid earthquakes of a certain magnitude (Gauchner et al. 2015).

From research on induced seismicity, it can be concluded that the majority of earthquakes are located on larger faults; however, the transport of fluid induced deformations may be considered permeability and porosity dependent. This work investigates numerically by means of the Finite Element Method (FEM) the influence of a) homogeneous poroelastic medium, b) a heterogeneous poroelastic medium containing small-sized defects, and c) a hydraulic fracture within a poroelastic medium on the stability of a fault system during simultaneous depletion and injection.

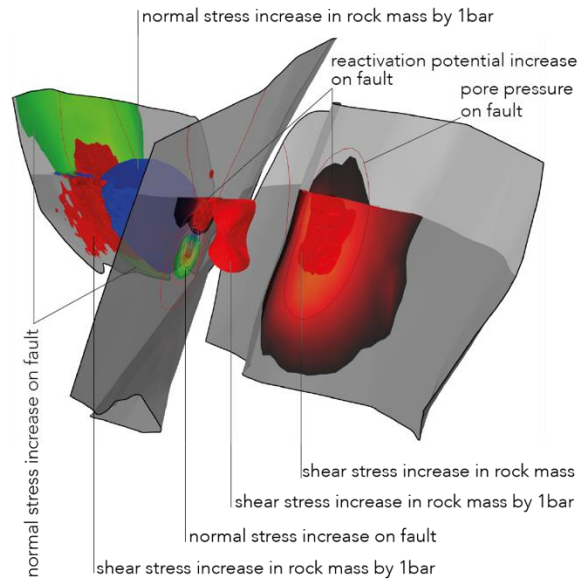
Figure 19 shows the model and results. It can be seen that instability on faults occur irrespective of the modelling approach at the same locations of the faults, but the magnitudes may be different.

The presented workflow for THM coupled simulations of the geomechanical system behaviour for hydrocarbon or geothermal reservoirs is capable to incorporate complex geometries and geomechanical models. It can be employed to analyse and optimise the effect of operation and stimulation of such a reservoir on rock mass stability, rock mass permeability enhancement, spatial and temporal distribution of stresses and porosity, and resulting fault stability. The model building may be complemented with upscaled and hence realistic rock mass parameters. Relating the destabilised areas on faults with empirical relationships to seismic magnitudes may be a way forward to gain confidence in public.

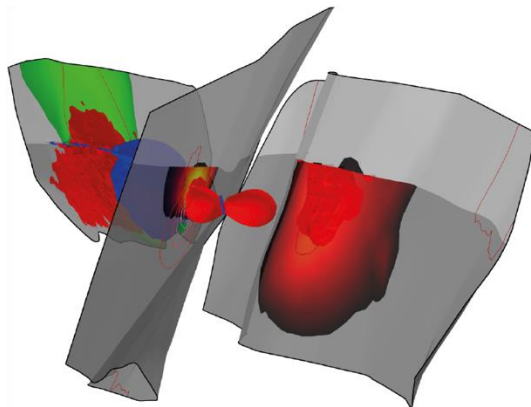
MODEL



RESULT POROELASTIC SOLUTION



RESULT FRACTURE NETWORK



RESULT HYDRAULIC FRACTURE

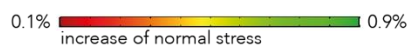
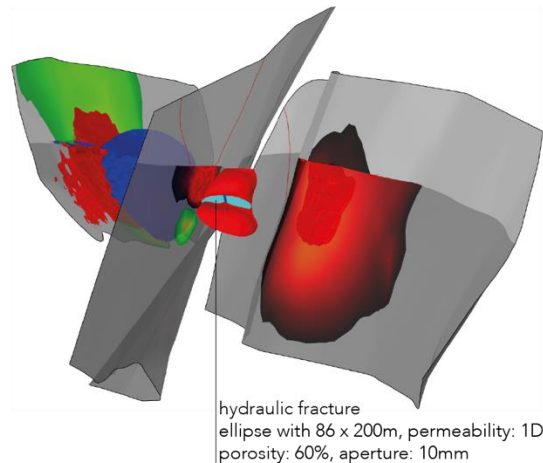


Figure 19: [top left] Model for the numerical simulations. The model consists of a cap- (light grey on faults) and a reservoir rock mass (dark grey) that are cut by permeable faults. Injection of cold water is applied through an open hole section in the southern compartment (blue line) while production is conducted in the northern compartment (red line). [top right] Results of the simulation with poroelastic rock mass. Large areas of the southern fault become destabilised during injection (red), while the northern fault is stabilised by production (green). Stability on the faults is not aligned with pore pressure (isolines). The rock mass shows some increase in differential stresses at the injection well and close to the faults (red isobar). In the production compartment large volumes get depressurised as indicated by the blue isobar. [bottom left] Results from simulation with a non-homogeneous fracture containing rock mass highlight reduced areas of stability change on faults. [bottom right] The results of simulation of the influence of a hydraulic fracture treatment show comparable fault stability pattern compared to the homogeneous solution (top right) but with altered influence on rock mass.

3.4.3 Next steps and social impacts

The results have been and will be published in scientific journals, presented at conferences and meetings, used in lecturing and made public in social networks. The team members will

use them in their daily scientific and commercial work. The industrial partner will incorporate the results in their business workflows.

The results will be the basis for another EU funded project, namely S4CE (Science for Clean Energy, Project Number 764810), where the routines developed here can be used to understand and predict seismic hazard and related permeability evolution.

The results will help to better plan and optimise projects not only in shale gas exploitation but also conventional and geothermal applications.

3.4.4 Selected publications resulting from this work

Apostolopoulou M, Day R, Hull R, Stamatakis M and Striolo A. 2017. A kinetic Monte Carlo approach to study fluid transport in pore networks. *JCP*, 147 (134703), 1–10.

Apostolopoulou M, Dusterhoft R, Day R, Stamatakis M, Coppens M-O and Striolo A. in prep. Estimating Permeability in Heterogeneous Porous Media: Deterministic and Stochastic Investigations.

Meier T, Grühser C and Backers T. 2018. Workflow For Homogenising Permeability Of A Low Permeable Rock Containing A High Permeable Discrete Fracture Network. 80th EAGE Conference and Exhibition 2018. DOI: 10.3997/2214-4609.201801635.

Meier T and Backers T. 2018. Reactivation of Fault Zones due to Thermo-Poroelastic Stress Changes. 80th EAGE Conference and Exhibition 2018. DOI: 10.3997/2214-4609.201800715.

Phan A, Cole DR, Wei RG, Dzubiella J and Striolo A. 2016. Confined Water Determines Transport Properties of Guest Molecules in Narrow Pores. *ACS Nano*, vol. 10, no. 8, pp. 7646–7656.

Porter RTJ, Meier T, Grühser C, Backers T, Striolo A. in prep. Numerical simulations of permeability enhancement during hydraulic fracturing using extended finite element and non-linear diffusion models.

3.4.5 References

Gaucher, E., Schoenball, M., Heidbach, O., Zang, A., Fokker, P. A., Van Wees, J. D., and Kohl, T. [2015] Induced seismicity in geothermal reservoirs: A review of forecasting approaches. *Renewable and Sustainable Energy Reviews*, **52**, 1473–1490.

Grotzinger J and Jordan T. 2017. *Press/Siever, Understanding Earth*. Springer Nature.

King, G. C. P., Stein, R. S., and Lin, J. [1994] Static Stress Changes and the Triggering of Earthquakes. *Bulletin of the Seismological Society of America*, **84**(3), 935–953.

Moeck, I. and Backers, T. [2011] Moeck I, Backers T. 2011. The fault reactivation potential as critical factor in reservoir utilization. *first break*. 29 (5): 73 - 80.

Shapiro, S. A. [2015] Fluid-induced seismicity. Cambridge University Press

Wells, D. L., and Coppersmith, K. J. [1994] New Empirical Relationships among Magnitude, Rupture Length, Rupture Width, Rupture Area, and Surface Displacement. *Bulletin of the Seismological Society of America*, **84**(4), 974–1002.

Zoback, M. D. [2010] Reservoir geomechanics. Cambridge University Press.

3.5 Synthesis and Characterisation of Engineered Materials

3.5.1 Scientific questions and environmental impacts addressed

WP7 focused on the synthesis, characterization and understanding the properties of novel porous materials, in particular zeolites, with regard to the adsorption of methane and carbon dioxide. Porous materials, zeolites as typical representatives of natural microporous materials, are common in the nature and understanding of their behavior as for the adsorption and transport of methane and carbon dioxide are directly related to this topic of the ShaleXenvironment project (SXT).

More specifically, to get a better insight into the behavior of shale gas in reality to make some model, in optimum case, having predictable value, it is important to prepare well-defined materials. For that purpose we have synthesized series of zeolite, which are microporous crystalline materials with precisely defined sizes of their micropores. These were not only those already known in the literature but also we have applied our own new procedure called ADOR (for details see below).

To understand the behavior of fluids in the well-defined pores, we have investigated two approaches, i) combined adsorption and diffusion study of light alkanes using computer simulations, and ii) adsorption of carbon dioxide in the series of isorecticular zeolites.

3.5.2 Main results achieved during the project

From the synthetic point of view we have examined the general synthetic pathway for the synthesis of novel zeolites as depicted in **Figure 20**. The ADOR method developed in our laboratory utilizes oriented chemical weakness of some bonds (in our particular case of Ge-O bonds) to selectively disassemble the parent zeolite and to form the layered material. In this project we succeeded to use zeolite **UOV** and to transform it into another new zeolite **IPC-12**.

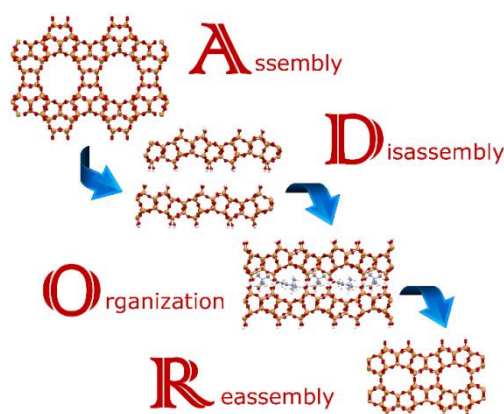


Figure 20: Schematic representation of ADOR process. ‘A’ stands for assembly of the parent UTL structure, ‘D’ – disassembly to IPC-1P zeolite precursor, ‘O’ – organizing by intercalation of organics, and ‘R’ – reassembly by calcination (in this example to IPC-4 (PCR)).

Successful synthesis of IPC-12 is important step forward in the synthesis of zeolites as this was the second example how to disassemble the parent zeolite and to produce another one. It strongly evidences the general applicability of ADOR mechanism, which in the future surely will not be limited to zeolites.

Using Monte Carlo and molecular dynamics simulations, we predicted adsorption isotherms and transport diffusivities of light alkanes in microporous and hierarchical ZSM-5 zeolites. The hierarchical ZSM-5 zeolite with dual micro/mesoporosities was modeled as an MFI structure where a cylindrical mesopore of 4 nm diameter was introduced. All isotherms were type I, except for propane and n-butane in the dual-porosity zeolite, which were type II. In the dual-porosity zeolite, methane was preferentially adsorbed in the zeolite micropores rather than in the mesopores. Analogous behavior occurred for ethane up to a crossover pressure. With increasing number of carbon atoms for propane and n-butane, the crossover shifted to lower pressures, and the uptake in the dual-porosity zeolite became higher than the uptake in the microporous zeolite. This was due to the multi-interaction sites in ethane, propane, and n-butane molecules, which increased the adsorbate-pore surface interactions and led to an enhancement in the adsorption of these alkanes in the zeolite mesopores. Unlike in the microporous zeolite, the self-diffusivity for methane, ethane, and propane increased with the pressure. Introducing transport mesopores into the MFI structure also had a tremendous effect on the transport of the alkanes in the dual-porosity zeolite. When compared to the microporous zeolite, the collective diffusivity increased by about 1 to nearly 2 orders of magnitude, and except for n-butane, the collective diffusivity is higher than the self-diffusivity.

We have investigated a series of isorecticular zeolites (those having the same structure of layers but different connectivity) in carbon dioxide adsorption, **Figure 21**).

These zeolites were prepared by ADOR method, with exception of UTL zeolite, and were in purely siliceous form. X-ray diffraction, transmission electron microscopy and argon adsorption isotherms confirmed a high crystallinity and quality of these materials.

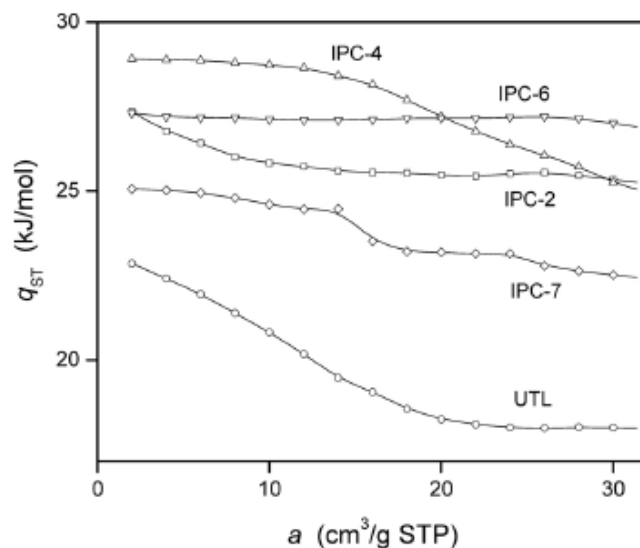


Figure 21: Isosteric heats of adsorption of carbon dioxide on UTL and IPC-n zeolites.

The experimental study of temperature dependence of carbon dioxide adsorption provided a detailed information on the interaction of carbon dioxide with siliceous surface of channels of these isorecticular zeolites. In accordance with domination of dispersion interactions of carbon dioxide with zeolites under study, it was clearly evidenced that determined isosteric adsorption heats depend primarily at low surface coverages on the channel width. At higher surface coverages lateral interactions of CO₂ molecules contribute to adsorption heat, **Figure 21**. As a result, in contrast to other types of adsorbents, these isorecticular zeolites exhibit rather “flat” dependences of isosteric heats on the adsorbed amount of CO₂, which could be interesting for relatively easy regeneration.

Obtained dependences of the adsorption heat of CO₂ on the amount adsorbed are more sensitive to the microporous structure than single adsorption isotherms, *i.e.* than the dependences of amount adsorbed on equilibrium pressure. The profiles of adsorption heat facilitate to discriminate channel systems in the zeolite.

Relationship between isosteric adsorption heats of carbon dioxide and the morphology of zeolite channels was determined. It was shown that the isosteric adsorption heat characterizes the structure features of IPC-n zeolites with a higher resolution than adsorption isotherms.

3.5.3 Next steps and social impacts

The team members will continue in the development of the zeolite synthesis and characterization of prepared materials to better understand their adsorption/separation properties.

In addition, they will continue to disseminate the knowledges acquired in this work package to other colleagues and students in the frame of Symposia/Workshops and teaching courses at the Charles University. Presentations for some industrial partners are also envisaged.

3.5.4 Selected publications resulting from this work

1. Expansion of the ADOR Strategy for the Synthesis of Zeolites: The Synthesis of IPC-12 from Zeolite UOV
Kasneryk, V; Shamzhy, M; Opanasenko, M; Wheatley, PS; Morris, SA; Russell, SE; Mayoral, A; Trachta, M; Cejka, J; Morris, RE
ANGEWANDTE CHEMIE-INTERNATIONAL EDITION 56, 2017, 4324-4327
2. Adsorption and Diffusion of C-1 to C-4 Alkanes in Dual-Porosity Zeolites by Molecular Simulations
Rezlerova, E; Zupal, A; Cejka, J; Siperstein, FR; Brennan, JK; Lisal, M
LANGMUIR 33, 2017, 11126-11137
3. The effect of pore size dimensions in isorecticular zeolites on carbon dioxide adsorption heats
Zupal, A; Shamzhy, M; Kubu, M; Cejka, J
JOURNAL OF CO₂ UTILIZATION, 24, 2018, 157-163

3.6 Optimisation of Shale Gas Water Treatment

3.6.1 Introduction and Objectives

The objective of WP08 was to develop an **optimization model for the shale gas water management** that takes into account all the aspects relevant to the water usage in the shale gas extraction to assist all the 'actors' involved to make the best decisions. The model should take simultaneously into account:

- a) Economic factors such as, fresh water acquisition, transport, storage, drilling, etc.
- b) Environmental impacts such as fresh water consumption, waste water recovery (by using the a zero liquid discharge (ZLD) approach).
- c) social impacts like employment, economic effects on the local community, health and safety, Nuisance (noise and traffic), public and media perception, etc.

Additionally, a more detailed analysis of the environmental impacts of the wastewater treatment in Shale Gas Extraction has been carried out through a generic Life Cycle Assessment (LCA) and the ReCiPe metric. To that end it was necessary to identify and characterize fresh water sources. A particular well pad has different water necessities for drilling and fracking activities. Forecast of water necessities and regulations related to fresh water source must be taken into account to effectively minimize both costs and environmental impacts related to the acquisition, transport and fresh water storage before its use.

After drilling and stimulating activities are completed, a fraction of the water injected returns to the surface as 'flowback water', typically between 24-40% during the first 2-4 weeks (although in some cases it can even surpass the 100%). After this period, the flow presents a fast decline and stabilizes in flows below 1 m³/h ('produced water'). This water could contain a large number of contaminants. Among these, the most important ones to take into account are *Total Dissolved Solids (TDS)*, *Total Suspended Solids (TSS)*, *Bacteria*, *Organics*, *Hardness* that is a description of the concentration of scale forming ions (Calcium, magnesium, Barium, Strontium), *Oil and Grease*, *Normally Occurring Radioactive Material (NORM)*. Produced water typically contains small amounts of radioactive materials found naturally in shale formations. Radium isotopes (²²⁶Ra and ²²⁸Ra) are most important due to their higher solubility. In general, NORM does not appear in remarkable amounts in flowback produced water. In any case, if they appear they should be precipitated and removed.

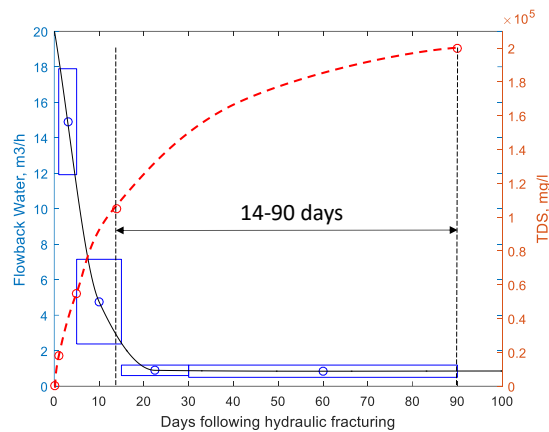


Figure 22: Typical profile of water flow and TDS vs time. Based on data from Marcellus Shale (USA)

The major challenge in the treatment of the shale water, is to deal with *Total Dissolved Solids* (TDS) that could range between 10 kg/m^3 and 200 kg/m^3 , with a typical value around 70 kg/m^3 that tends to increase with time. This very high salinity requires specific treatments especially tailored to Shale Gas water. Thus, the major challenge in the treatment of shale gas water is simultaneously deal with a decaying flow and an increasing salinity (**Figure 22** shows the typical behavior of flowback flow and salinity).

3.6.2 Optimal Shale Water Pre-Treatment

Depending on its final destination, the water must undergo a different set of treatments that are designed depending on the wastewater physicochemical characteristics and on the requirements of the final desalination treatment selected. In general, water must undergo a set of initial pre-treatments to remove some components (TSS, divalent and trivalent ions, organics, microorganisms, etc.) and/or to prepare the water for the following desalination treatment. In this context «pre-treatment» can be defined as the set of treatments that flowback water must undergo before desalination. This definition include also all the treatments is desalination could be eventually not necessary for instance, in the case of direct re-use of the wastewater.

We developed a superstructure optimization based approach [1] that allows determining the optimal structural configuration and operating conditions for the pre-treatment of the shale gas waste water, taking into account different alternatives of water uses and desalination process (such as membrane or thermal technologies). The superstructure is staged based. In the first stage, the best alternative for removing large particles (filtration). The second stage removes small particles (if necessary) or simply send the water to the next stage where it is decided how to remove colloidal particles and scale forming ions (coagulation/precipitation, electrocoagulation, flocculation). In the fourth stage, particles formed in previous one are removed by sedimentation, dissolved air flotation or granular filtration. Then the water is disinfected and if needed some extra treatment could be necessary (e.g. ultrafiltration) especially if desalination is carried out with membrane based technologies.

3.6.3 Shale Water Desalination

From an economic point of view, the state of the art in seawater desalination is reverse osmosis (RO). However, RO is constrained to TDS lower than ~40,000 – 45,000 mg/L. For higher salinities it is necessary to use thermal desalination. Thermal desalination has been widely used in seawater desalination, however there are important differences: In seawater desalination the objective is to obtain fresh water, but in shale gas the wastewater is a byproduct and therefore the objective is treating the water for different reuses (internal reuse, irrigation, disposal) reducing at much as possible the final liquid waste. In seawater desalination, the rejected water must have low salinity (lower than 50,000 mg/L – 60,000 mg/L) and it is usually returned back to the sea. In the case of shale gas wastewater, the objective is to be as close as possible to Zero Liquid Discharge. In sea water desalination it is possible to use a large excess of water, for example cooling purposes and reject it directly to the sea, but in shale gas the water is scarce. In consequence, even though some thermal technologies have been adapted to the shale gas wastewater treatment, the adaptation is not straightforward. Among the available thermal (or hybrid membrane/thermal) alternatives we have deeply studied Multiple-effect evaporation with mechanical vapor recompression (MEE-MVR) and membrane distillation (MD).

MEE-MVR. Using a superstructure based optimization we performed a comprehensive study of the optimal structural and operation characteristics of the MEE-MVR systems [2-4]. Some conclusions were: The optimal number of evaporation stages depends on the salinity, but a design with two stages and a single vapor recompression is optimal in most of the situations. Results showed that the size is small enough to be built on mobile units (trucks) that can be easily transported for on-site operations. In the case of uncertainty in flow (and salinity) is still possible to develop efficient units, however in this case it is necessary to use a low grade external source of heat (low pressure steam). However, this is not difficult in a shale play where there are usually flares from which residual heat can be recovered. The cost is around 6.5-12 \$/m³ of treated water with a residual brine close to salt saturation.

MD. Membrane distillation is a promising technology that combines the advantages of thermal based and membrane based processes. Even though, as far as we know there are no MD systems operating in actual plants, and the technology deserved a comprehensive optimization to evaluate its potential capabilities. In MD the separation occurs across a hydrophobic semipermeable membrane below the normal boiling point of the inlet stream. This feature offers a great potential for using MD operations with waste heat. This option is especially advantageous in remote unconventional hydrocarbon extraction sites where electrical energy supply is not available and many waste heating sources are present, such as flares. Furthermore, MD is also very attractive for this application due to its mobility and modularity.

Using Direct Contact Membrane Modules we have developed a stage based superstructure that allows determining the optimal membrane modules configuration and the operating conditions for shale gas water desalination. The solution shows that MD is both technically

feasible and economically a competitive with costs around 10-14 \$/m³ of treated water. MD could be really interesting if in the shale play there are a free low grade energy source (*e.g.* residual energy from a flare that are common in gas exploitations). In this case MD presents the lower investment costs and it must be an alternative to take into account.

3.6.4 Shale Water Management

In order to effectively exploit a shale play, it is crucial to coordinate all the activities with the objective of maximize the benefits while, at the same time, attempt to minimize the environmental impacts and obtain the social approval (*i.e.* to get that the shale gas activities be perceived as a benefit to the society). To that end, we developed a comprehensive multi-period management model that takes into account all the operational aspects involved in the shale gas water management. We have developed a superstructure based multi-period planning model that can be virtually adapted to any shale gas exploitation in the world. It takes into account:

- Available fresh water sources to supply the water for hydraulic fracturing operations, the water withdrawal cost and constraints about water availability (maximum amount of water that can be withdraw –taking into account regulations about minimum caudal, ecological water reserves, local regulations, etc.)
- The capacity and the maximum number of freshwater tanks available to store the water required to complete each well.
- A set of shale gas wells belonging to a specific wellpad including water requirements, fracturing time and crews available to perform the drilling and completion phase. Forecasts for the profiles for the flowback flowrate, TDS concentration and gas production curve per well.
- The capacity and the maximum number of fracturing tanks to store the wastewater. Each storage unit includes the cost associated to move, demobilize and clean out the tanks before removing it from the location and leasing cost.
- A set of Class II disposal wells to inject the wastewater and the corresponding cost of disposal. In general in this project we did not take into account this possibility, mainly because it is unlike that in Europe this practice be approved, but it has been included by completeness.
- A set of treatment technologies to desalinate the flowback water onsite. The maximum capacity, treatment cost, leasing cost and the cost associated to move, demobilize and clean out are also given. Previous work in WP08 provided detailed information or rigorous models to estimate the related cost in different scenarios.
- A set of centralized water treatment (CWT) plants and the treatment cost and maximum capacity of each facility.
- Locations of freshwater source, centralized water treatment (CWT), disposal wells and wellpads.
- Transportation costs of freshwater and wastewater via trucks.

- The cost of moving rigs, well drilling and completion, shale gas production and friction reducers.
- The forecast of sales price of shale gas per week for all prospective wells must also be known.

The objective function consists of maximizing the «Sustainable Profit». Sustainable profit includes economic profit, eco-costs and social profit. The **economic profit** includes revenues from natural gas minus the sum of the following expenses: drilling and production cost, wastewater disposal cost, storage tank cost, freshwater cost, friction reducer cost, wastewater and freshwater transport cost and onsite and offsite treatment cost. **Eco-cost** is a robust indicator from cradle-to-cradle LCA calculations in the circular economy that includes eco-costs of human health, ecosystems, resource depletion and global warming. Finally, the **Social profit** includes social security contributions paid for the employed people to fracture a well, plus the social transfer by hiring people, minus social cost.

Results shows that, in general, the optimal coordination of activities in a single wellpad or in different closed wellpads allows increasing a lot the water re-use (e.g. in a typical case the freshwater consumption can be reduced in more than 40%). Reduction in costs are mainly due to an optimal water acquisition, transport and eventually final treatment of produced water and their corresponding eco-cost.

3.6.5 Life Cycle Assessment

Using as starting point the previous results of WP08, as well as the results from WP10 (Life Cycle Assessment) we carried out a detailed inventory of impacts (LCI) and a Life Cycle Impact Assessment (LCIA) of all the activities related with the water management in general, and the desalination treatments in particular. Detailed information can be found in the WP08 Deliverable 8.1. As an example, **Figure 23a** shows the environmental impacts of each one of the main stages of the shale gas production, while **Figure 23b** presents the comparison of the environmental impacts of each damage subcategory for the different desalination technologies studied. In both cases, by using the end point level in the ReCiPe metric.

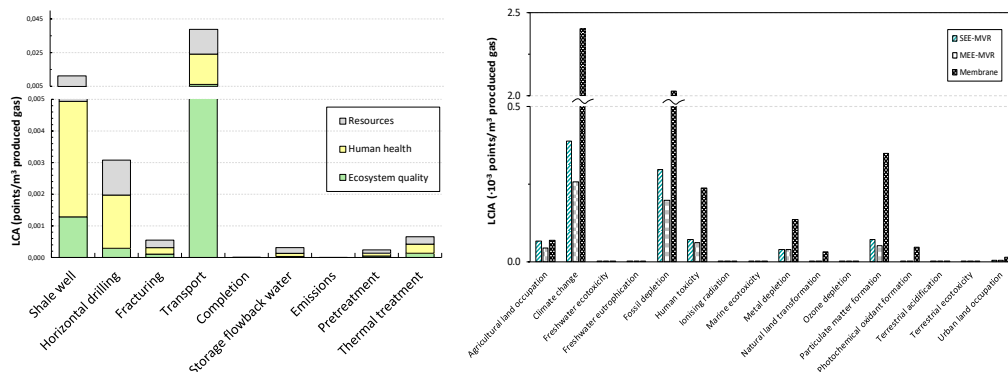


Figure 23: a) Environmental impacts by section for the extraction of shale gas. b) Comparison of the environmental impacts of the studied desalination technologies by damage subcategory.

3.6.6 Next Steps and social impacts

The models developed in this project have proved to be a valuable tool to help the designers to take the best decisions in all the aspects related to the water utilization in shale gas exploitation. With an approximate forecast of evolution of the flow and the physicochemical characteristics of the shale gas wastewater it is possible to use the proposed models to take the best decisions about the water treatment(s) needed (including pre-treatment options and water desalination alternatives). Besides, the water management model can be used for determining how much fresh water is needed, when and where acquire that water, when start and end the hydraulic fracking of each well, with which crew, what is the size of the fresh and waste water tanks, when and how much water must be reused in other wells (or even in other wellpads) when and how much waste water treat, etc.

The optimal results show that: It is possible to reduce the costs of the water desalination systems maintaining the close to ZLD philosophy. The correct coordination of fracking scheduling with water reuse allows reducing the freshwater consumption and therefore all the costs and environmental impacts related to acquisition, transport and treatment.

The models developed are flexible enough to be used in virtually all situations (USA, Europe, China, etc.). Their major drawback is the quality of the information needed (*i.e.* it is expected that the forecasts in the well-known exploitations in USA produce better results than those in Europe). In relation with this drawback, the next step consists of extending the model to deal with uncertainty in the most important parameters mainly the flow (*e.g.* optimal actions to take if the flow of flowback water is lower than expected and there are no water enough to fracture the 'next well').

Additionally, the cooperation in all the water management activities between companies working close each other (sharing transport, storage, reusing water between well-pads, etc.) has also a large potential. Some preliminary results have shown important reductions in total costs (an environmental charges) with benefits for all the parties. Application of Cooperative game theory concepts has proved to be a promising way of dealing with this problem and it is currently under development.

3.6.7 Selected publications resulting from this work

- [1] A. Carrero-Parreño, V.C. Onishi, R. Salcedo-Díaz, R. Ruiz-Femenia, E.S. Fraga, J.A. Caballero, J.A. Reyes-Labarta, Optimal Pretreatment System of Flowback Water from Shale Gas Production, *Ind. Eng. Chem. Res.* 56 (2017) 4386–4398.
- [2] V.C. Onishi, A. Carrero-Parreño, J.A. Reyes-Labarta, E.S. Fraga, J.A. Caballero, Desalination of shale gas produced water: A rigorous design approach for zero-liquid discharge evaporation systems, *J. Clean. Prod.* 140 (2017)
- [3] V.C. Onishi, A. Carrero-Parreño, J.A. Reyes-Labarta, R. Ruiz-Femenia, R. Salcedo-Díaz, E.S. Fraga, J.A. Caballero, Shale gas flowback water desalination: Single vs multiple-effect evaporation with vapor recompression cycle and thermal integration, *Desalination.* 404 (2017) 230–248.

[4] V.C. Onishi, R. Ruiz-Femenia, R. Salcedo-Díaz, A. Carrero-Parreño, J.A. Reyes-Labarta, E.S. Fraga, J.A. Caballero, Process optimization for zero-liquid discharge desalination of shale gas flowback water under uncertainty, *J. Clean. Prod.* 164 (2017) 1219–1238. doi:10.1016/j.jclepro.2017.06.243.

3.7 Development of a reliable wellhead blowout model and its applicability to a case study

3.7.1 *Scientific questions and environmental impacts addressed*

Safety and environmental risks associated with exploration and exploitation of the shale gas resources can be related to induced seismicity caused by hydraulic fracturing, and also to well failures and blowouts at the exploration stage during drilling into shale formationsⁱⁱⁱ. Fluids lost from a well during a blowout can also result in environmental damages, with in some cases significant remediation costs. In this part of the project, we have focused on evaluation of safety hazards of shale gas wells, aiming to provide modelling tools for use at the design stage to ensure best protection of near-by population and people working on the site.

To ensure accurate evaluation of safety hazards we have focused on coupling of models predicting explosion and jet fire consequences of a well blowout, with a transient computational flow model simulating transient discharge from the well during uncontrolled release.

3.7.2 *Main results achieved during the project*

The models developed enable full and accurate characterisation of safety hazards and evaluation of safe distances to people and structures as a part of risk assessment of a shale gas exploration/production site. We have demonstrated effectiveness of the model in a case study based on realistic design of a shale gas exploration site. The simulation model predictions are presented in the form of 2D plots of thermal radiation and explosion over-pressure contours as a function of distance and time following well blowout. This data in turn forms the basis for determining the minimum safety distances taking into account defined thresholds for deferent severity harm scenarios. **Figure 24** shows the instantaneous incident heat flux radiation contours at the ground level within +/- 200 m from the jet flame at 0.5, 2, 10 and 50 seconds after the well blowout. The results correspond to zero wind speed and 200 bar formation pressure. It can be clearly seen that the incident heat flux decreases with the distance from the centre of the jet and also decays with the time, reaching its maximum of ca 3 kW/m² at ca. 20 m distance from the well at time interval of 30 s.

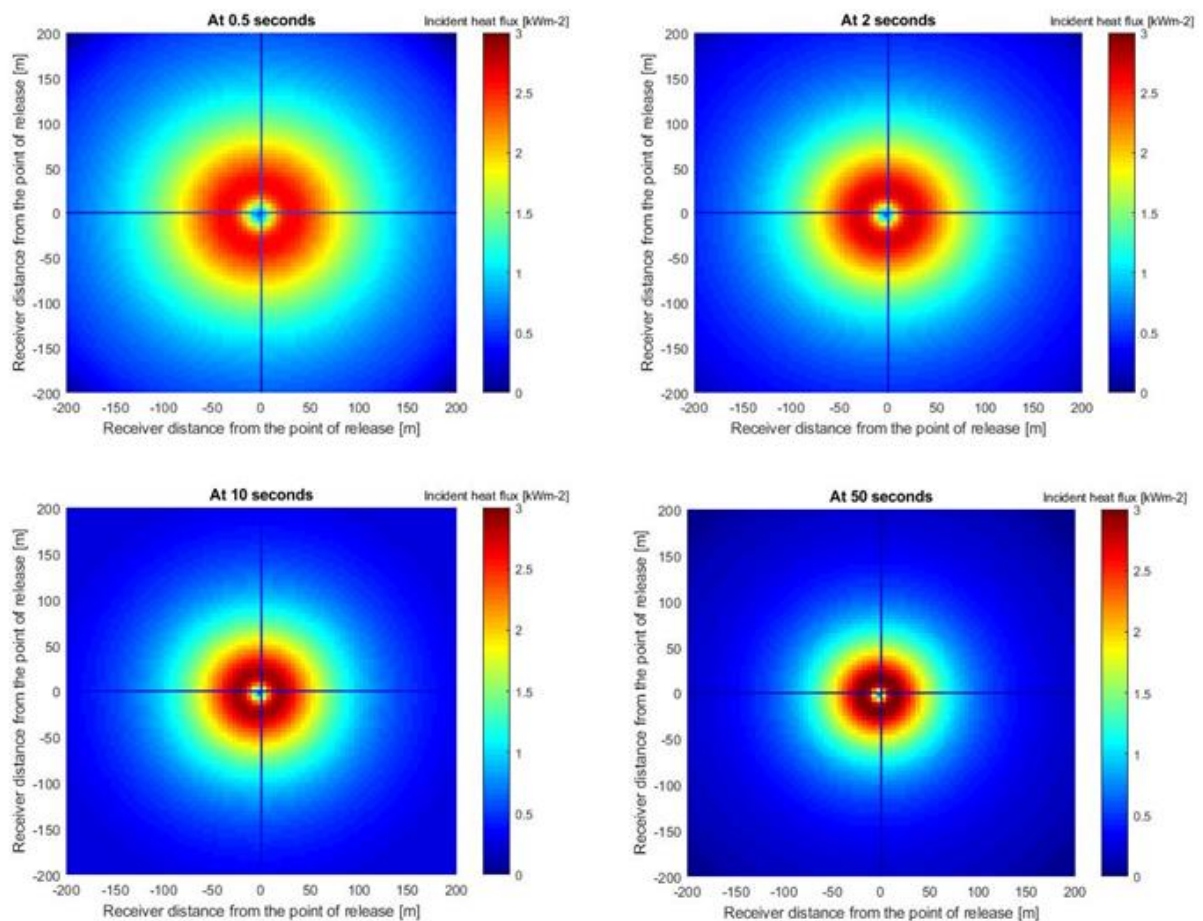


Figure 24: Incident heat flux contours at the ground level around vertical flame formed from the wellhead, predicted at 0.5, 2, 10 and 50 seconds following blowout under no wind conditions.

3.7.3 Next steps and social impacts

The models developed can be incorporated in a general methodology evaluating various environmental, safety and economic risks of shale gas projects. In terms of physical hardware, blowout risk-prediction capabilities can be enhanced through the use of bottom-hole detection systems to prevent gas kicks.

The methodology developed can be recommended for safety assessment of shale gas production facilities to ensure safe design and minimal risks to personnel and population.

3.7.4 Selected publications resulting from this work

Title: Multiphase CFD modelling of thermal radiation as a result of fires following a well blowout during shale gas production.

Abstract: The European Union currently imports ca. 50% of the natural gas it uses, and every year it must seek new gas contracts. Because conventional oil reserves are diminishing and renewable energy sources are in general not yet able to provide sufficient and affordable energy consistently at large scale, shale formations have the potential of providing large sources of gas for decades to come. However, it is critically important that the design and

operation of shale gas facilities meet the required safety standards for minimising or eliminating the risks to the environment and society.

3.8 Development of a Methodology for quantifying the likelihood of natural and induced seismic activity due to hydraulic fracturing and its application to case studies

3.8.1 *Scientific questions and environmental impacts addressed*

In this work package, methodologies to assess the risk of induced seismicity during reservoir stimulations are developed and applied to case studies. These methodologies are computational, and hence mathematical modelling techniques are used to simulate fluid injection into a reservoir and quantify the seismic response based on the reservoir's characteristics.

The methodologies are applicable to hydraulic fracturing of shale gas reservoirs during the fluid injection stage and also during the “shut-in” period afterwards when the flow into the reservoir is stopped. Possible causes of induced seismicity in hydraulic fracturing of low permeability rock formations are illustrated in **Figure 25**. Firstly, levels of micro-seismicity that are too weak to be felt at the surface are generated during the creation of fractures in the rocks themselves. These events are part of the hydraulic fracturing process, which induces the formation of fracture networks to enhance fluid transport in the sub-surface. For the triggering of events that are strong enough to be felt at the surface, several scenarios are possible, which could generate a permeable pathway between the fluid injection point and a pre-existing fault. Direct fault activation may occur when a hydraulic fracture directly intersects a pre-existing fault. Indirect activation could be triggered by diffusion of pore pressure away from the injection zone along local faults and fractures. Additionally, faults may be activated if injection wells are drilled directly into them, via fluid flow through existing fractures, through more permeable rock strata above or below shale formations, or through bedding planes that interface the rock strata (Davies et al., 2013). Even in the circumstances when stimulated fractures and the fracturing fluids may be hydraulically isolated from any pre-existing faults. The fault may in fact be activated through perturbations in the stress field brought about by changes in volume or mass loading transmitted to the fault poroelastically (right, **Figure 25**). The developed robust predictive methodologies can be used as preliminary assessment of the risk of induced seismicity for given geological conditions and injection parameters such as volumetric rates and pressures. They could also be coupled to seismic monitoring techniques during the fluid injection operations for the adaptive adjustment of seismic safety margins in relation to the seismic response of a reservoir. These methodologies can therefore contribute to the lowering of induced seismicity risk and reduce the frequency of occurrence.

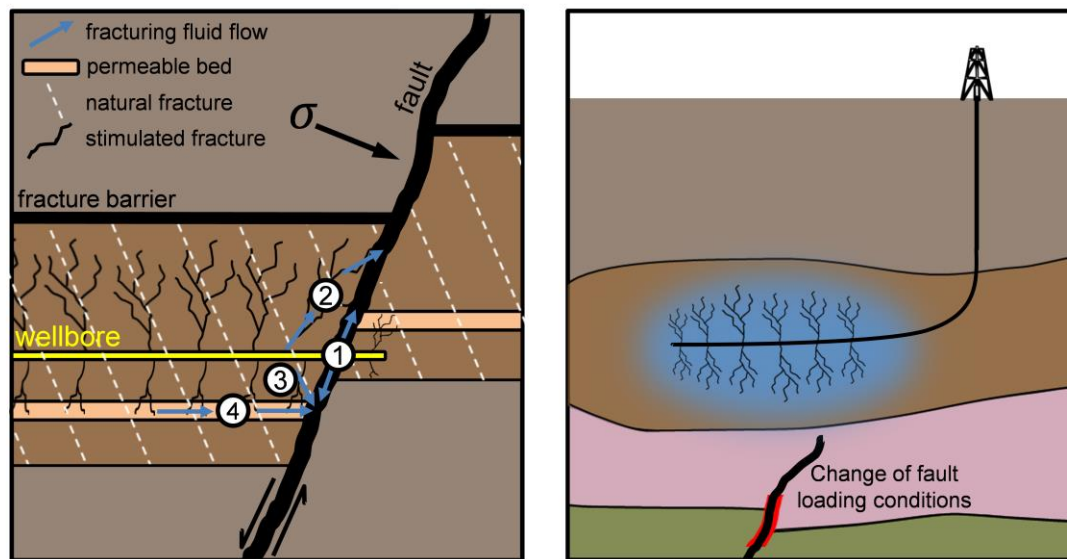


Figure 25: Physical mechanisms that could induce seismicity in hydraulic fracturing, (left): 1) Injection well drilled directly into fault, 2) hydraulic fracture directly intersects fault, 3) fluid flow through existing fractures, 4) through more permeable rock strata above or below shale formations, or through bedding planes that interface the rock strata; (right) changes in the stress field brought about by changes in volume or mass loading transmitted to the fault proelastically (After Davies et al., 2013 and Schultz et al., 2017).

3.8.2 Main results achieved during the project

During the project, coupled reservoir flow and geomechanical models for computer simulation of sub-surface fluid injections and fault reactivation for a given site characterisation were developed. The reservoir models for fluid flow are used to predict subsurface pressure changes during and after injection. The reservoir flow models are based on the numerical solution of sets of finite-difference equations that describe transient, multi-phase flow in heterogeneous porous media. Analytical solutions were obtained for different types of reservoir and injection conditions. With a prediction of pore pressure changes from the reservoir model, the potential to induce seismicity is then assessed using geomechanical models of faults, which can predict their propensity for slip. The model was applied to European case studies of induced seismicity for Bowland Shale and also to an Enhanced Geothermal System in Basel, Switzerland. For a given set of model input parameters, the model was able to reproduce the observed seismicity satisfactorily.

3.8.3 Next steps and social impacts

Future work in this area will entail, performing uncertainty analysis to understand how variation in input parameters can impact the model prediction. Currently the models are set-up in a one-dimensional framework but the dimensionality could be increased for increased sophistication and the ability to model the heterogeneity of the reservoir and the characteristics of known faults from seismic surveys.

Negative public perception to induced seismicity is a potential hazard for sub-surface energy operations with numerous international projections having been suspended, delayed or curtailed because of local public opposition. Both the public and policy makers hold

misconceptions about induced seismicity and these coupled with a lack of knowledge may influence risk and benefit perception of sub-surface energy technologies. A technically robust, transparent and balanced dialogue between industries, regulators, the public and other stakeholders can help to resolve misconceptions and risk perception issues. The developed computational models for risk assessment that are capable of predicting the conditions of the injection reservoir could be an important component in facilitating this dialogue. The research is also expected to contribute to the minimisation of induced seismic risks.

3.8.4 Selected publications resulting from this work

Title: Addressing the risks of induced seismicity in sub-surface energy operations

Abstract: Shale gas could help address the insatiable global demand for energy. However, in addition to risks of environmental pollution, the risk of induced seismicity during the hydraulic fracturing process is often considered as the major showstopper in the public acceptability of shale gas as an alternative source of fossil fuel. Other types of sub-surface energy development have also demonstrated similar induced seismicity risks. This article presents an interdisciplinary review of notable cases of suspected induced seismicity relating to sub-surface energy operations, covering operations for hydraulic fracturing, wastewater injection, conventional gas extraction, enhanced geothermal systems and water impoundment. Possible causal mechanisms of induced seismicity are described and illustrated, then methods to mitigate induced seismicity, encompassing regulations, including so-called traffic light systems, monitoring and assessment, and numerical modelling approaches for predicting the occurrence of induced seismicity are outlined. Issues relating to public perception of energy technologies in regards to induced seismicity potential are also discussed.

3.8.5 References

Schultz, R., Wang, R., Gu, Y.J., Haug, K., & Atkinson, G. (2017). A seismological overview of the induced earthquakes in the Duvernay play near Fox Creek, Alberta. *Journal of Geophysical Research: Solid Earth*, 122, 492–505. doi:10.1002/2016JB013570.

Davies, R.J., Foulger, G., Bindley, A., & Styles, P. (2013). Induced seismicity and hydraulic fracturing for the recovery of hydrocarbons. *Marine and Petroleum Geology*, 45, 171-185. <https://doi.org/10.1016/j.marpetgeo.2013.03.016>

3.9 Life Cycle Assessment and Shale Gas

3.9.1 What is Life Cycle Assessment?

Life Cycle Assessment (LCA) is a structured, comprehensive and internationally standardised approach for assessing the environmental impacts of products¹. It quantifies all relevant emissions and resources consumed, and the related environmental and health impacts and resource depletion issues taking into account the full life cycle of a product: from the extraction of resources, through production, use, and recycling, up to the disposal of remaining waste.

The approach has many applications. It has primarily been developed to aid decisions, but other applications such as marketing, supporting the development of new policies or assessing already implemented policies and decisions ex-post are also very common. The European Commission has more than once asserted that LCA represents the best tool for assessing the environmental impacts of products and policies. It has established the European Platform on Life Cycle Assessment (EPLCA) to support business and government needs for availability and quality of life-cycle data and studies (<https://bit.ly/2IbuRV2>), and has developed the International Reference Life Cycle Data System (ILCD) to provide a common basis for consistent, robust and quality-assured life-cycle data and studies (JRC, 2010).

3.9.2 Why Life Cycle Assessment?

The very first reason, which sets LCA apart from other approaches, is that LCA adopts a holistic and comprehensive perspective in terms of processes included and environmental issues covered. As noted above, LCA takes into account the full life-cycle of products from cradle to grave, but it also considers a wide range of environmental issue including global warming, freshwater use, acidification, depletion of non-renewable resources, impacts of toxic on humans and the ecosystems, and many others. This perspective primarily enables LCA to identify trade-offs, in terms of shifting burdens between phases of the life cycle or problems between different impact categories, when evaluating decisions or comparing alternative products. For instance, the decision to substitute steel with aluminium for car frames would shift burdens from the use phase of cars (because steel is heavier, it consumes more fuel) to the manufacturing phase (the production of aluminium is more energy-intensive than that of steel), but also environment problems from global warming (from vehicles exhaust emissions) to toxic impacts to humans and ecosystems (associated with aluminium production). It must be noted that the comprehensiveness of LCA is affected by two major limitations: first, LCA requires a considerable amount of data to cover all the processes that are part of the life cycle, and second, LCA requires simplifications and generalisation in the modelling of environmental impacts that prevent LCA from calculating actual impacts (instead, it calculates potential impacts).

¹ Here, the term product is used to refer to both goods and services.

A strength of LCA is that its results are quantitative in the sense they are able to answer questions such as “how much does a product system potentially impact the environment ?” The quantitative nature of LCA means that it can be used to compare environmental impacts of different systems, for example with the aim of judging which products are better for the environment or to point out those processes that contribute the most to the overall impact, and therefore should receive most of the attention. It must be noted that while LCA can tell which product is better for the environment, it cannot tell whether that product is “good enough”. It is thus wrong to declare that a product is environmentally sustainable in absolute terms based on LCA results, which tend to be comparative.

3.9.3 Life Cycle Assessment and shale gas

Let us discuss why LCA should be applied to shale gas. Energy policies are based on three core dimensions – energy security, energy cost and (primarily environmental) sustainability. Energy policy-makers in all countries aim to achieve the same three objectives: maximising security of supply, minimising cost, and minimising environmental impacts. These three policy goals constitute a ‘trilemma’, entailing complex, interwoven links between public and private actors, governments and regulators, economic and social factors, national resources, environmental concerns and individual behaviours. Delivering policies, which simultaneously address energy security, the cost of energy and socially and environmentally sensitive production and use of energy is arguably one of the most formidable challenges facing government and industry.

Because shale gas is an indigenous resource, much less concentrated than conventional fossil fuels and even conventional resources of uranium, it can contribute to increasing the security of supply of countries with no or little fossil reserves and under-exploited renewable energies. However, the cost of shale gas and its potential to positively affect global and domestic gas and electricity prices remains still uncertain; it appears promising, but more practical experience is required before reaching definitive conclusions. To support the case for shale gas extraction and use, its environmental impacts, especially relative to other energy sources, must be quantified and analysed to determine its environmental sustainability, with a special focus on greenhouse gas emission. The LCA provides the most appropriate tool for this task.

3.9.4 The LCA standard framework

The fundamental structure of LCA has been established by the ISO in 1997 and has since remained unchanged. **Figure 26** shows the LCA standard framework (ISO, 2006a, 2006b) which consists of the following four phases:

1. Goal and Scope Definition;
2. Life Cycle Inventory analysis (LCI);
3. Life Cycle Impact Assessment (LCIA);
4. Life Cycle Interpretation.

The ISO standards clearly highlight the iterative nature of LCA in the sense that earlier phases may be revisited in light of the results of later phases. For instance, changes in the material input to a manufacturing process or changes in the process itself may trigger the need to update the inventory component; whilst new information about the impact of substances on the environment will require the Impact Assessment to be updated.

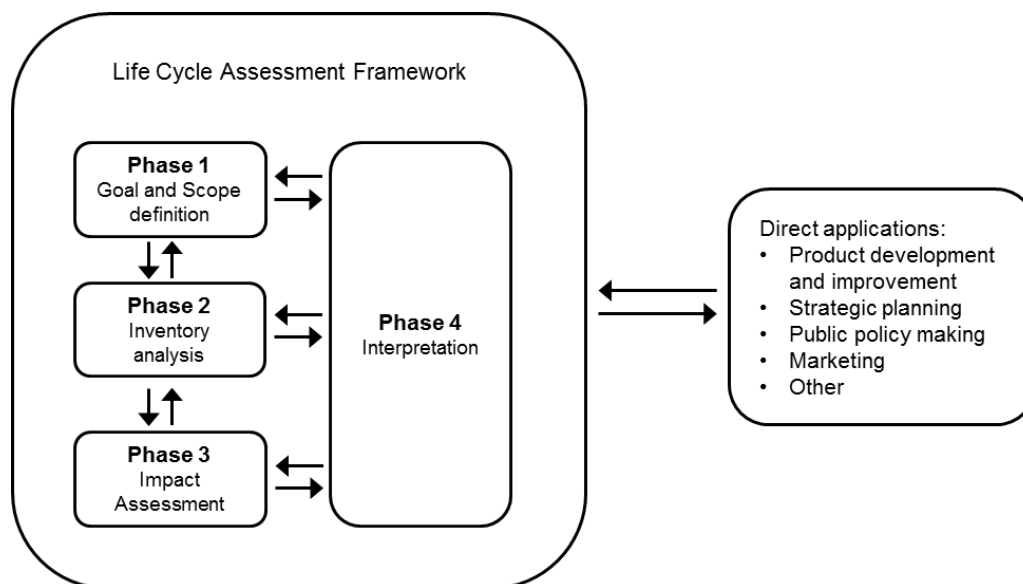


Figure 26: Phases of Life cycle Assessment, adapted from ISO 14040 (ISO, 2006a).

3.9.4.1 Goal and Scope definition

The very first step of any LCA envisages the definition of the goal of the study, which primarily has to include: i) the intended application of the study; ii) the reason for carrying it out; iii) the intended audience (which affects the technical level of reporting and the interpretation of results); and iv) the commissioner of the study, to highlight potential conflicts of interests.

In the case of shale gas, LCA studies can be used i) to compare the environmental performance of shale gas as source of heat or electricity with conventional fossil and alternative sources, ii) to identify the phases of the life cycle that contribute the most to the environmental impacts, thus recommending potential improvements, and also iii) to support governments in the development of new domestic policies, for instance, for tackling climate change. The reasons for carrying out the study can thus be to support decisions (*e.g.* in developing policies), learning about the environmental impacts of shale gas or about the effect of implemented policies, or to support technical improvements. The intended audience can range from policy-makers (in developing policies) to the general public (*e.g.* for ex-post policy assessment) to technical people working in the shale gas life cycle (for identification of hot-spots and possible improvements).

The definition of the scope of the study has to address two main aspects:

- It has to provide a quantified description of the function to be satisfied by the product under study, namely the Functional Unit, and a quantified amount of the product necessary to deliver the function, namely the reference flow.
- It has to specify the boundary of the product system in terms of all the processes that are to be included (see **Figure 27**).

Essentially, there are two alternative approaches to perform LCA (these are also called “modes”), which affect the system boundary as well as the life cycle inventory modelling. The attributional approach analyses a single existing or hypothetical product system, to address the question “what environmental impact can be associated with this product?”. The consequential approach, on the other hand, aims to describe indirect changes outside the immediate product system induced by changes in production rates. The former is appropriate as the basis for environmental product labelling, as well as for aiding decisions that are not deemed to cause structural changes; whilst the latter has been specifically developed to deal with large scale decisions that can cause structural changes. The definition of consequential LCA, thus, imply that the system boundary is expanded to include those processes that are affected by the decisions under study. Some procedures have been developed to aid in the identification of such processes (*e.g.* see Weidema et al., 1999)

Shale gas can in effect perform two functions: it can act as a source of electricity or heat. The functional unit can be defined as the production of 1 kWh of electricity or 1 MJ of heat generated, and the reference flow is represented by the amount of shale gas required to produce 1 kWh of electricity or 1 MJ. Notably, the definition of the function and of the functional unit is essential in comparative studies because they represent the basis on which the comparison is performed.

Figure 27 shows the system boundary for shale gas production developed within the SXT project. The study did not investigate any decisions; thus, the attributional approach has been adopted. As it is common practice in LCA, the system boundary is divided into two sub-systems: the foreground system includes all the processes that can be affected by decisions based on the study, whilst the background system includes all the other processes that supply materials, water and energy to the foreground system. Because the extraction of shale gas includes many activities that are in common with conventional gas, it may be advantageous to subdivide the foreground system into processes that are generic or specific to shale gas (these are termed conventional production and hydraulic fracturing in Figure 27). The subdivision can help in the collection of data as well as in the interpretation of the results. The distinction between foreground and background also guides the procedure of data collection: primary data, defined as high-quality data either measured directly at the plant site, or derived from measurements, process flowsheets or questionnaire compiled by people with technical knowledge of the process, is to be used for the foreground system;

whilst secondary data, which represent lower quality data or less specific data, is to be used for the background.

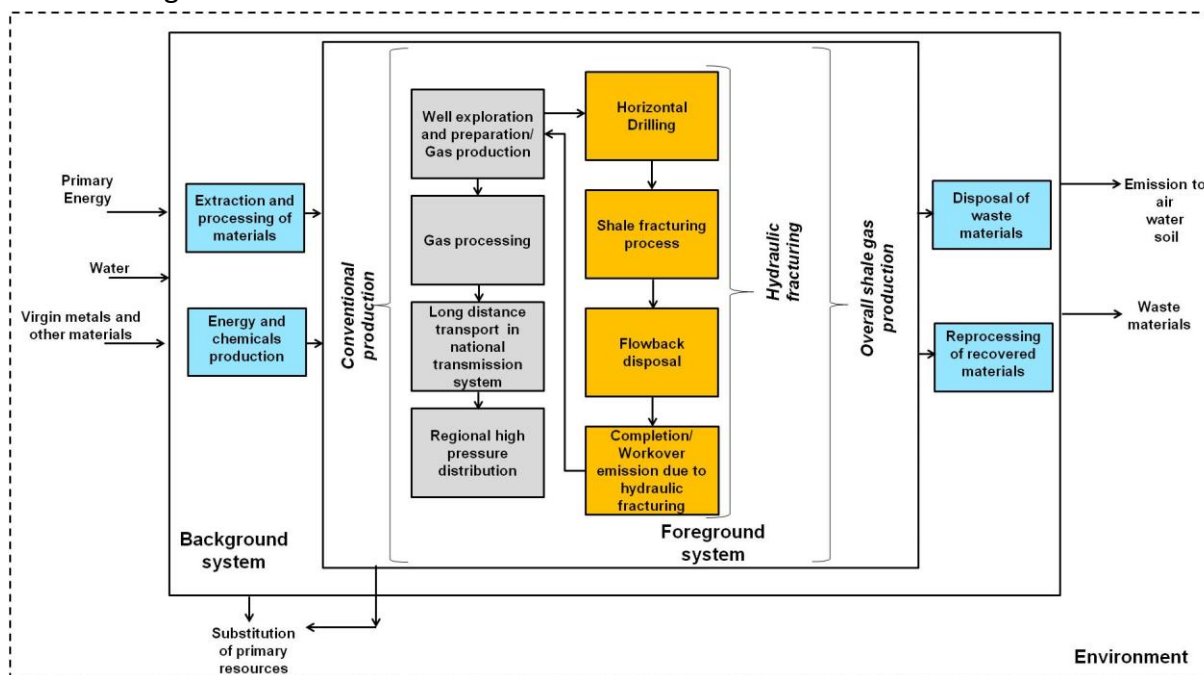


Figure 27: System boundary for shale gas within the SXT project. Yellow boxes represent the hydraulic fracturing process, grey boxes identify the conventional processes and the blue boxes refer to the activities of the background system.

The consequential approach should be adopted when the goal of the study is to investigate the effect of international or national policies or decisions aimed at increasing the production of shale gas. In this case, structural changes to the industry are in fact to be expected, and thus the system boundary needs to include those processes that are deemed to be affected. For instance, the increase in production and use of shale gas would replace an equivalent form of electricity or heating; the most likely candidate would be carbon or conventional natural gas.

3.9.4.2 Life Cycle Inventory

The Life Cycle Inventory (LCI) phase consists of two main steps: i) collection of data for all the process units included in the system boundaries, and ii) calculation procedures to quantify relevant inputs and outputs of the product system. The LCI result is a list of quantified elementary flows² and represents the input for the next phase .

It is recommended to collect primary data only for the foreground system; whilst secondary data can be used for the background system and for those processes of the foreground system for which primary data is not available. Secondary data can be obtained from commercial databases like Ecoinvent (Wernet et al., 2016) and Gabi (PE International, 2012).

² Elementary flows are defined as those flows that cross the system boundaries either as input or output; emissions to atmosphere and water bodies, water and virgin materials are notable examples.

One of the most debated issues in LCA concerns the allocation of environmental impacts to processes delivering multiple functions. A heat and power cogeneration unit is a notable example of a multifunctional process. How can the total environmental impacts of producing specific amounts of electricity and heat be allocated only to electricity? (For instance, this could be useful if electricity for pumping drilling fluid is supplied by a cogeneration unit.) The ISO standards (ISO, 2006a, 2006b) include a hierarchical approach to deal with multifunctional processes: first, the process should be subdivided into sub—processes, each linked to only one function; if subdivision is not possible, system expansion or crediting should be used. The former is used for comparative studies where the product system is compared with other systems that provide the same functions. The latter is used for standalone studies: the product system is credited for the secondary functions by subtracting the environmental impacts associated with an alternative process that delivers such function. Finally, if neither subdivision nor system expansion/crediting can be used, the environmental impacts should be partitioned between the functions using physical or economic relations.

Multifunctionality is unlikely to represent a major issue in LCA studies concerning shale gas. As noted above, shale gas can act as a source of heat or electricity. In a standalone study where shale gas is burnt in heat and power cogeneration unit, the environmental impacts of either electricity or heat can be quantified by crediting the product system with the most likely alternative of producing either function, represented respectively by the country grid mix for electricity or heating. No other major processes in the production of shale gas should feature major allocation issues.

3.9.4.3 Life Cycle Impact Assessment

The Life Cycle Impact Assessment (LCIA) phase essentially involves two tasks: i) selection of impact categories, category indicators and characterisation models; and ii) calculation of the category indicator results.

An impact category is defined as a class of environmental issues to which Life Cycle Inventory (LCI) results may be assigned, whilst category indicators are a quantifiable representation of impact categories. Characterisation models describe the environmental mechanisms that link the LCI results and the category indicators; they are used to derive characterisation factors, which effectively translate LCI results to the common unit of the category indicator. Category indicator results are the summation of the impact of all species to a specific impact category.

Table 1: Examples of LCIA terms (adapted from ISO, 2006a))

| Term | Example |
|----------------------------|--|
| Impact category | Climate change |
| LCI results | Amount of a greenhouse gas per functional unit |
| Characterization model | Baseline model of 100 years of the Intergovernmental Panel on Climate Change` |
| Category Indicator | Infrared radiative force (W/m ²) |
| Characterization factor | Global warming potential (GWP ₁₀₀) for each greenhouse gas (kg CO ₂ -equivalent/kg gas) |
| Category Indicator results | Kilograms of CO ₂ -equivalents per functional unit |

The selection of impact categories should reflect as closely as possible those environmental issues that are related to the product system being studied. Two different types of impact categories indicators have been established: midpoint indicators are located early in the cause-effect chain and are the most commonly used; while endpoint indicators are located at the end of the cause-effect chain to represent impacts on one of the three Areas of Protection (AoP), namely Human Health, Ecosystems Quality or Nature Environment, and Natural Resources and Ecosystems Services. For each impact category, multiple characterisation models have been developed. These are usually collated in so-called impact assessment methods; ILCD (JRC, 2012, 2011), ReCiPe (Goedkoop et al., 2013) and CML (Guinée et al., 2002) are some of the most used ones.

In practice, the LCIA phase, including the calculation of the category indicator results, is nowadays largely automated and requires the practitioner to choose an LCIA method, and few other settings via menus and buttons in an LCA software. Gabi (<https://bit.ly/2vtJezc>) and Simapro (<https://bit.ly/2Ozph2q>) are some of the most used commercial software, whilst openLCA (<https://bit.ly/2m3z6qN>) represents a free alternative.

With respect to shale gas, the selection of relevant impact categories must indeed include global warming. This is because, with increasing international pressure to curb greenhouse gas emissions, the introduction of new fuels into national grid mix must be supported by environmental claims that primarily demonstrate the potential of the fuel to achieve national and international targets. Other relevant impact categories include: consumption of non-renewable materials, particularly significant in hydraulic fracturing activities, and toxic impacts to humans and ecosystems, which are mainly associated with the disposal of the drilling fluid. For LCA studies applied to the European context, it is recommended the use of the ILCD impact assessment method, developed by the Joint Research Centre (JRC) of the European Union following a review of several impact assessment methods and characterisation models. The method developed at the Institute for Environmental Science (CML) at Leiden University represents a frequently used alternative.

3.9.4.4 Life Cycle Interpretation

Life Cycle Interpretation is the last phase of the LCA standard framework which aims at analysing the results of the other phases to develop conclusions and recommendations that respect the intentions of the goal of the study. The interpretation should present the conclusions of the LCA in an understandable way and help the users of the study appraise their robustness and potential weaknesses in light of any identified limitations.

The life cycle interpretation should primarily comprise the three following elements:

- Identification of significant issues, intended as those elements that have the potential to change significantly the final results of the LCA study. These may include inventory data, impact categories and individual process units or groups of processes that have significant contributions to LCI or LCIA results. In comparative studies, this step should also focus on the analysis of how the environmental profiles of the compared systems differ.
- Sensitivity and uncertainty analysis, which have the purpose of assessing the reliability of the final results. When possible, it is recommended to perform both sensitivity and uncertainty analysis. The former aims at assessing how sensitive are the results with respect to changes in inputs, such as inventory data; whilst the purpose of the latter is to evaluate how much each input parameters contributes to the output variance.
- Conclusions and final recommendations based on the outcomes of the other phases of LCA. In this step it is essential to verify that conclusions are in accordance with the goal and scope of the study, and in particular with data quality requirements, assumptions, limitations of the study and application-oriented requirements. Based on final conclusions, recommendations related with the intended application of the study should be developed.

The Life Cycle Interpretation phase is highly specific to each LCA study. In the SXT project, the interpretation of results has demonstrated that shale gas-specific activities have relatively minor impacts compared to activities in common with natural extraction and production (*e.g.* see **Figure 28** which refers to the global warming category). Thus, shale gas and natural gas are expected to have very similar environmental impacts.

Furthermore, the sensitivity analysis (see **Figure 29**) has highlighted that the Estimated Ultimate Recovery (EUR) of shale gas wells is a key parameter to which LCA results are highly sensitive. The analysis thus recommends that major efforts should be concentrated on collecting highest possible quality of data for such parameter. The uncertainty analysis would have given a more compelling picture by identifying those parameters that not only are very sensitive, but also that are very uncertain. However, performing uncertainty analyses is much more problematic because further data on the variance and distribution of model parameters has to be collected; often, such information is not available.

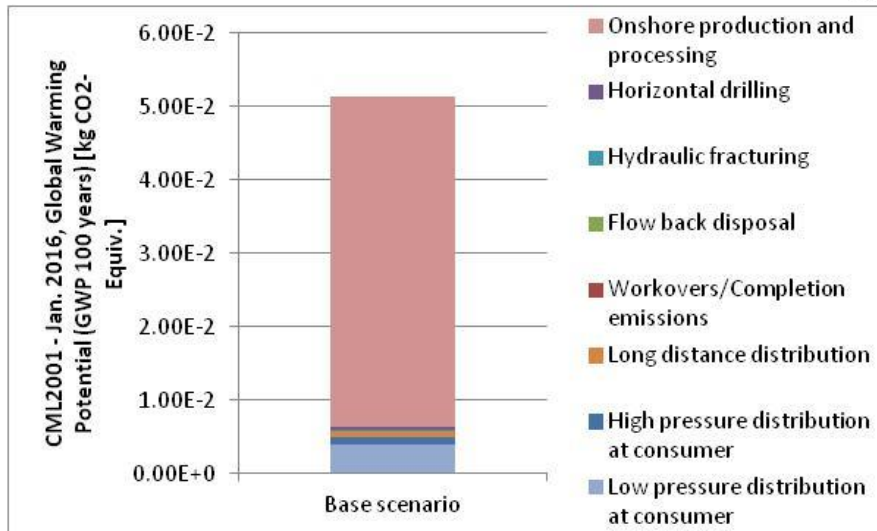


Figure 28: Hot-spot analysis for the global warming category relative to the production of 1 MJ of shale gas.

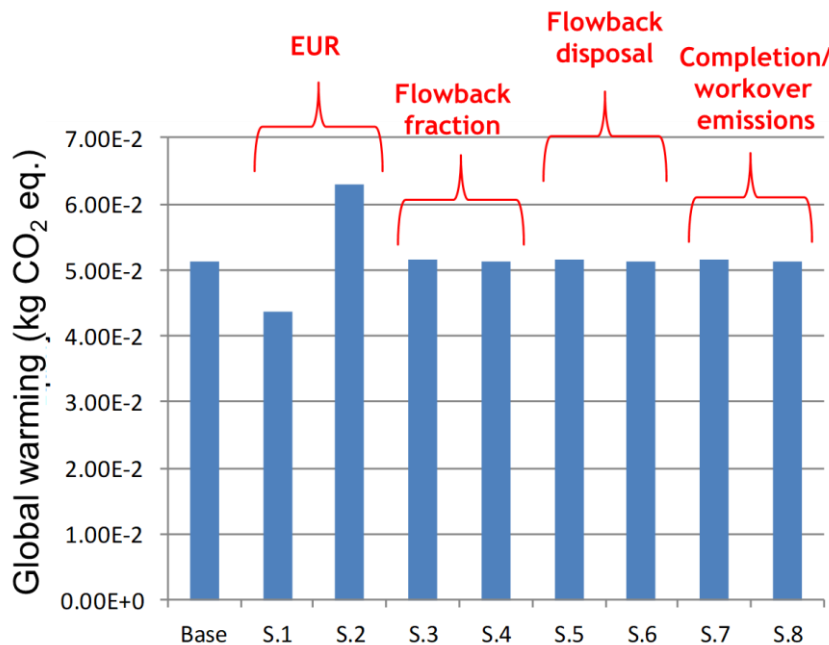


Figure 29: Sensitivity analysis for the global warming category relative to the production of 1 MJ of shale gas.

3.9.5 Reading material

Pedagogical books and reports

- Baumann, H., Tillman, A.M., 2004. The Hitch Hiker’s Guide to LCA: An orientation in life cycle assessment methodology and application. Studentlitteratur, Lund, Sweden. doi:10.1065/lca2006.02.008
- Hauschild, M.Z., Rosenbaum, R.K., Olsen, S.I., 2017. Life Cycle Assessment: Theory and Practice. Springer International Publishing. doi:10.1007/978-3-319-56475-3
- JRC, 2010. ILCD Handbook - General guide for Life Cycle Assessment - Detailed guidance. doi:10.2788/38479

LCA studies on shale gas

- Cooper, J., Stamford, L., Azapagic, A., 2014. Environmental Impacts of Shale Gas in

the UK: Current Situation and Future Scenarios. *Energy Technol.* 2, 1012–1026. doi:10.1002/ente.201402097

- Tagliaferri, C., Clift, R., Lettieri, P., Chapman, C., 2017. Shale gas: a life-cycle perspective for UK production. *Int. J. Life Cycle Assess.* 22, 919–937. doi:10.1007/s11367-016-1207-5

3.9.6 References

- Goedkoop, M., Heijungs, R., Huijbregts, M.A.J., De Schryver, A., Struijs, J., van Zelm, R., 2013. ReCiPe 2008. A life cycle impact assessment method which comprises harmonised category indicators at the midpoint and the endpoint level. First edition (revised). Report I: Characterisation.
- Guinée, J.B., Gorrée, M., Heijungs, R., Huppes, G., Kleijn, R., de Koning, A., van Oers, L.F.C.M., Sleeswijk, A.W., Suh, S., Udo de Haes, H.A., de Bruijn, H., van Duin, R., Huijbregts, M.A.J., 2002. *Handbook on Life Cycle Assessment. Operational Guide to the ISO Standards.* Kluwer Academic Publishers, Dordrecht.
- ISO, 2006a. *Environmental Management - Life Cycle Assessment - Principles and Framework.* EN ISO 14040:2006.
- ISO, 2006b. *Environmental Management - Life Cycle Assessment - Requirements and guidelines.* EN ISO 14044:2006.
- JRC, 2012. *Characterisation factors of the ILCD Recommended Life Cycle Impact Assessment methods: database and supporting information,* European Commission. European Commission Joint Research Centre. doi:10.2788/60825
- JRC, 2011. *Recommendations for Life Cycle Impact Assessment in the European context - based on existing environmental impact assessment models and factors.* doi:10.278/33030
- JRC, 2010. *ILCD Handbook - General guide for Life Cycle Assessment - Detailed guidance.* doi:10.2788/38479
- PE International, 2012. *GaBi Database & Modelling Principles 2012 6.*
- Weidema, B., Frees, N., Nielsen, A.-M., 1999. Marginal production technologies for life cycle inventories. *Int. J. Life Cycle Assess.* 4, 48–56. doi:10.1007/BF02979395
- Wernet, G., Bauer, C., Steubing, B., Reinhard, J., Moreno-Ruiz, E., Weidema, B., 2016. The ecoinvent database version 3 (part I): overview and methodology. *Int. J. Life Cycle Assess.* 21, 1218–1230. doi:10.1007/s11367-016-1087-8

3.10 Worthiness and Social License to Operate (SL₂O)

Up until now but especially in the 20th century, the majority of decisions in the energy sector have been based on economic considerations. Today this attitude is changing towards a more holistic approach: sustainability is the underpinning concept and for natural resources like shale gas, stewardship.

Environment, economics and society represent the classical three pillars of sustainability. For each of them, a practical methodology based on the life-cycle perspective has been developed; these are Life Cycle Assessment (LCA), Life Cycle Costing (LCC) and Social Life Cycle Assessment (S-LCA), respectively concerned with the environmental, economic and social aspects. Life Cycle Assessment is the most developed and widespread life-cycle methodology; the EU has asserted in more than one occasion the LCA represents the best tool for assessing the environmental impacts of products or policies. Life Cycle Costing, but especially Social Life Cycle Assessment represent methodologies still under development. However, several initiatives or programmes are focusing on these aspects, and the number of LCC and S-LCA studies are on the rise.

How can the concept of sustainability be used to support local communities, decisions or policies? Is it possible to analyse whether a shale gas resource company or a shale gas technology has 'worthiness'? The integration of the three life-cycle methodologies allows a comprehensive evaluation of the sustainability profile of a product or operational technique, known as Life Cycle Sustainability Assessment. Based on the results of such a comprehensive investigation, the most sustainable option(s) should be regarded as the most preferred one(s).

But how are these methodologies integrated? Should they be simply summed one to another? Or should each score be weighed? And if so, which weighting should be used? Usually for decisions within the public sector, it is advised that both the criteria of the assessment (*i.e.* which categories or types of impacts should be quantified for each methodology) and the weights are to be elicited as part of the process.

We propose to demonstrate how a **Life Cycle Sustainability Assessment (LCSA)** can be used to support decisions on natural resource projects, such as shale gas, based on a weighted distribution of its corresponding **Worthiness**; a sort of 'Worthiness Index'. The work would consist in i) performing three life cycle studies, each focusing on one of the three aspects of sustainability (environment, economics and society), and ii) engaging with different groups of stakeholders, representative of different perspectives such as local communities, local investors and planners, environmental agencies, policy-makers and institutions, technical and commercial enterprise, to elicit the criteria as well as the weights.

The overall Worthiness of a project can then be used to help develop a framework to initiate dialogue between these different parties to firstly attempt to secure acceptance, and ultimately credibility for the natural resource enterprise being considered. By focusing on

‘matters of concern’ rather than ‘matters of fact’ (I.S. Stewart and D. Lewis, Communicating contested geoscience to the public: Moving from ‘matters of fact’ to ‘matters of concern’, Earth-Science Reviews 174 (2017) 122) will hopefully deliver a new form of Social License, a **Societal License to Operate (SL₂O)**. SL₂O will be addressing societal concerns over sustainability, traded off against the commercial benefits of enterprise, in-line with best practice technical stewardship of the associated natural resources. As the project develops through the various stage gates, the Worthiness of the project can be reassessed based on increasing local approval or enterprise awareness of local societal concerns.

4. Conclusions and future steps

The ShaleXenvironmentT consortium has implemented an holistic approach in an attempt to improve our understanding of shale gas and its production, quantify and reduce the risks associated with its exploration and production, and identify best practices for communicating with stakeholders. This deliverable contains summaries of the various activities conducted, which we believe could be used as a foundation for academic introductory courses on the subject matter. Some of this material is currently used in the post-graduate taught programme 'Global Management of Natural Resources', which was introduced by UCL in 2017. The programme currently attracts >20 students per year.

5. Publications resulting from the work described

A. Striolo, *Shale Gas: Friend or Foe?*, **The Chemical Engineer**, Issue 922, page 41, April **2018**.

ⁱ Willson, S. A Wellbore Stability Approach For Self-Killing Blowout Assessment. *SPE Deep. Drill. Complet. Conf.* **2012**, No. June, 20–21.

ⁱⁱ Duncan, I. Likelihood and Environmental Consequences of Blowouts of Shale Gas and Shale Oil Wells. **2016**, 9–11.